SC71033.FR

Copy No. 9

MOLTEN SALT ELECTRODEPOSITION OF HIGH TEMPERATURE SUPERCONDUCTORS

FINAL REPORT

September 7, 1990 to November 30, 1992

CONTRACT NO. N00014-90-C-0225

Prepared for:

Office of Naval Research
800 North Quincy Street
Arlington, VA 22217-5000

Prepared by:

D.M. Tench, M.W. Kendig and S. Jeanjaquet
Principal Investigator: D.M. Tench (805) 373-4509
Rockwell International Science Center
1049 Camino Dos Rios
Thousand Oaks, CA 91360

JUNE 1993

The views and conclusions contained in this document are those of the authors and should not be interpreted as necessarily representing the official policies, either expressed or implied, of the Defense Advanced Projects Agency of the U.S. Government.

Rockwell International
Science Center

REPORT SUMMARY

The overall objective of this project was to develop a process for direct electrodeposition of Y-Ba-Cu superconducting oxides from a molten salt at relatively low temperatures (300-550°C). An important finding was that cathodic deposition of metallic oxides, rather than free metals, generally occurs from nitrate melts, apparently via reduction of metal nitrato complexes. Oxide deposition was confirmed for Cu as CuO, Y as Y_2O_3, and Co as Co_3O_4, and apparently also occurs for Ba. Deposition of mixed Ba-Y-Cu oxides was demonstrated on both Cu and Pt substrates. Data were compiled that provide a good basis for designing schemes for deposition of various mixed oxides from nitrate melts. A sequential anodic injection method was conceived for depositing ultrathin mixed oxide layers, which can be viewed as an analog of molecular beam epitaxy. Results obtained with this approach were encouraging but were inconclusive because of contamination with Gd from the Y injection anode. Based on the results of this program and literature studies, cathodic metal oxide deposition from nitrate melts is a general phenomenon that could ultimately prove to be a practical means of preparing a variety of single and mixed anhydrous metal oxide films. It is recommended that future work focus initially on deposition of perovskite materials, which are of considerable practical interest and involve only two metallic components so that the required deposition schemes are inherently simpler.

INTRODUCTION

An intensive global effort is currently directed toward improving the quality of the new copper-oxide-based high-temperature superconductor (HTSC) materials that offer such exciting possibilities. The major problem is that low-temperature processing is needed for many practical applications but methods investigated to date do not yield materials of sufficient quality, even with the use of high-temperature sintering operations.

Under this program, we investigated the direct electrodeposition of the superconducting oxide itself from a molten salt in which the component species are dissolved. In this case, solid-state reactions and diffusional processes that invariably lead to high concentrations of defects and grain boundaries are avoided, and processing temperatures in the 200-600°C range are possible. In situ preparation allows exploitation of favorable reaction free energies to permit formation of ordered HTSC structures at the lowest possible temperature. Electrodeposition enables the addition of more energy in small increments and thus should further reduce the temperature required and provide precise control over the deposition process. This method is also applicable to irregular-shaped substrates and direct pattern deposition, and is readily scaled up or down.

One subtle but important feature of electrodeposition processes is a pronounced tendency toward formation of strong texture and large grains even on mismatched or disordered substrates. This is a consequence of the near-equilibrium deposition conditions attainable via electrical control, as opposed to thermal activation for which the depositing species typically arrive at the surface with considerable excess energy.

Attention in the present work was focused on deposition of Y-Ba-Cu layered oxides from an equimolar Na-K nitrate melt. The original concept was to directly electroform the required layered oxide structure via a judiciously chosen sequence involving cathodic depositions and anodic oxidations, possibly performed in concert with solution mass transport modulations designed to induce local variations in the melt composition. Thus, monolayer amounts of Cu or a copper oxide would be alternately electrodeposited and passivated to build up a layered oxide structure, and layers of other metallic oxides would be interspersed by electrodeposition or precipitation reactions. It was implicitly assumed that at least some of the constituents would be

deposited in the metallic state and the molten nitrate melt was chosen primarily because it offered exceptional control over the oxidizing power at the electrode surface.

TECHNICAL RESULTS

Most of the results of the present program are described in detail in the appended two papers, which have been submitted for publication in the Journal of the Electrochemical Society. In this section, the principal results are summarized and data not included in the publications are discussed. Unless otherwise noted, the melt was eutectic Na-K nitrate at 300°C, and potentials are always versus Ag/Ag^+ (0.07 M).

Copper Oxide Deposition

Because of the central role that copper plays in HTSC materials, its electrochemical behavior was investigated in some detail. By measuring the charge associated with dissolution of a known quantity of the metal at constant voltage, Cu was found to dissolve anodically in the melt in the 2+ oxidation state. From melts containing Cu^{2+} ion, cathodic deposition produces the oxide CuO, rather than the metal. This was verified by x-ray diffraction analysis of the deposit obtained on a Pt electrode. The deposition potential (0.25 V) is more than a volt positive of melt breakdown, indicating that a Cu nitrato complex that facilitates reduction of nitrate to oxide (and nitrite) is involved. Such a mechanism had previously been suggested, but not verified, for non-transition metals [1-4]. Based on Pt rotating disk studies, the deposition process is mass transport limited and the diffusion coefficient of complexed Cu^{2+} ion is 3.1×10^{-6} cm^2/s. Anodic stripping of CuO deposits is a complicated process that is apparently inhibited by adsorption of nitrite, rapid dissolution occurring only positive of 0.6 V.

Mixed Oxide Deposition

Yttrium was also shown by x-ray and Auger electron spectroscopy (AES) analysis to deposit cathodically as the oxide (Y_2O_3) rather than the metal. Barium apparently deposits as the oxide as well, but this was not verified. On oxidized Cu substrates, AES depth profiling results indicate that cathodic deposition from melts containing Y^{3+} results in mixed Cu-Y oxide compounds, having the nominal composition $Cu_{0.2}Y_{1.8}O_3$. In melts containing both Y^{3+} and Ba^{2+} ions, deposits obtained on oxidized Cu

electrodes were predominantly Y_2O_3, but the one obtained at a very negative potential (-1.0 V) contained 1-3 atom percent Ba distributed throughout the bulk surface oxide layer. These results indicate that mixed Y-Ba-Cu oxides can be deposited from the molten nitrate system.

Voltammetric Behavior of Individual Oxides

Figure 1 compares cyclic voltammograms at a Pt rotating disk electrode for melts containing either Cu^{2+}, Y^{3+} or Ba^{2+} ions. It is evident that in the absence of the other ions, deposition of Cu oxide would occur first on the Pt surface, then Y oxide, and finally the Ba species as the potential is decreased. Also, because of the overvoltage associated with stripping of the Y oxide deposit, deposition of an overlayer of CuO in the absence of other deposition processes would appear to be possible between 0.25 and -0.1 V. Likewise, codeposition of Cu and Y oxides in the absence of deposition of a Ba species appears possible between -0.1 and -1.2 V. However, for deposition of one material upon another or for codeposition, underpotential deposition and/or compound formation is likely to alter this picture considerably.

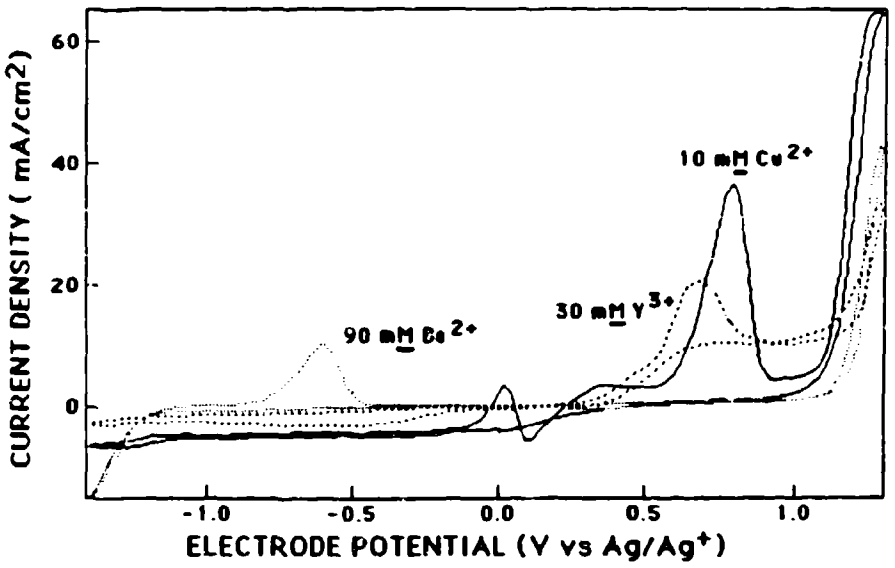

Fig. 1 Cyclic voltammograms (0.3 V/s) for a rotating Pt disk electrode (60 rpm) in eutectic Na-K nitrate melt (300°C) containing either 30 mM Y^{3+}, 10 mM Cu^{2+} or 90 mM Ba^{2+} ion.

Perovskite Possibilities

These data show that cathodic oxide deposition is a quite general phenomenon, which offers exciting possibilities for preparing a wide variety of single and mixed oxides. The likelihood that perovskites, specifically cobaltates, might be deposited from nitrate melts was established by demonstrating the deposition of cobalt oxide. The voltammetric behavior in this case is similar to that for Cu, with cathodic deposition beginning at 0.2 V. X-ray diffraction data showed that a black deposit obtained on a Pt rotating disk electrode at -0.75 V from a melt containing 50 mM Co ion (probably Co^{3+}) was Co_3O_4.

Oxide Deposition Considerations

Figure 2 summarizes the available onset potential data for the electrochemical reactions pertinent to metal oxide deposition from the eutectic Na-K nitrate melt References for the data taken from the literature are given in brackets. Onset voltages have been used to minimize ambiguities but a precision of better than ±0.1 V cannot be expected since values were sometimes taken from journal figures and reactant concentrations, solution mass transport, voltage sweep rates, and temperature were somewhat variable. Generally, data are for reactant concentrations between 20 and 100 mM, stationary or slowly rotating Pt electrodes (0-600 rpm), sweep rates of 0.3-0.5 V/s, and temperatures of 250-300°C (unless otherwise noted).

It is clear that the deposition potentials are sufficiently separated to permit metallic oxides to be selectively deposited in many cases. On the other hand, direct codeposition of some metallic oxides is also possible, particularly when compound formation occurs so that the potential for deposition of the more electropositive metal ion is shifted in the positive direction. This is apparently the case for Cu-Y oxides since Y is included in the Cu oxide at potentials positive of the Y deposition potential on platinum.

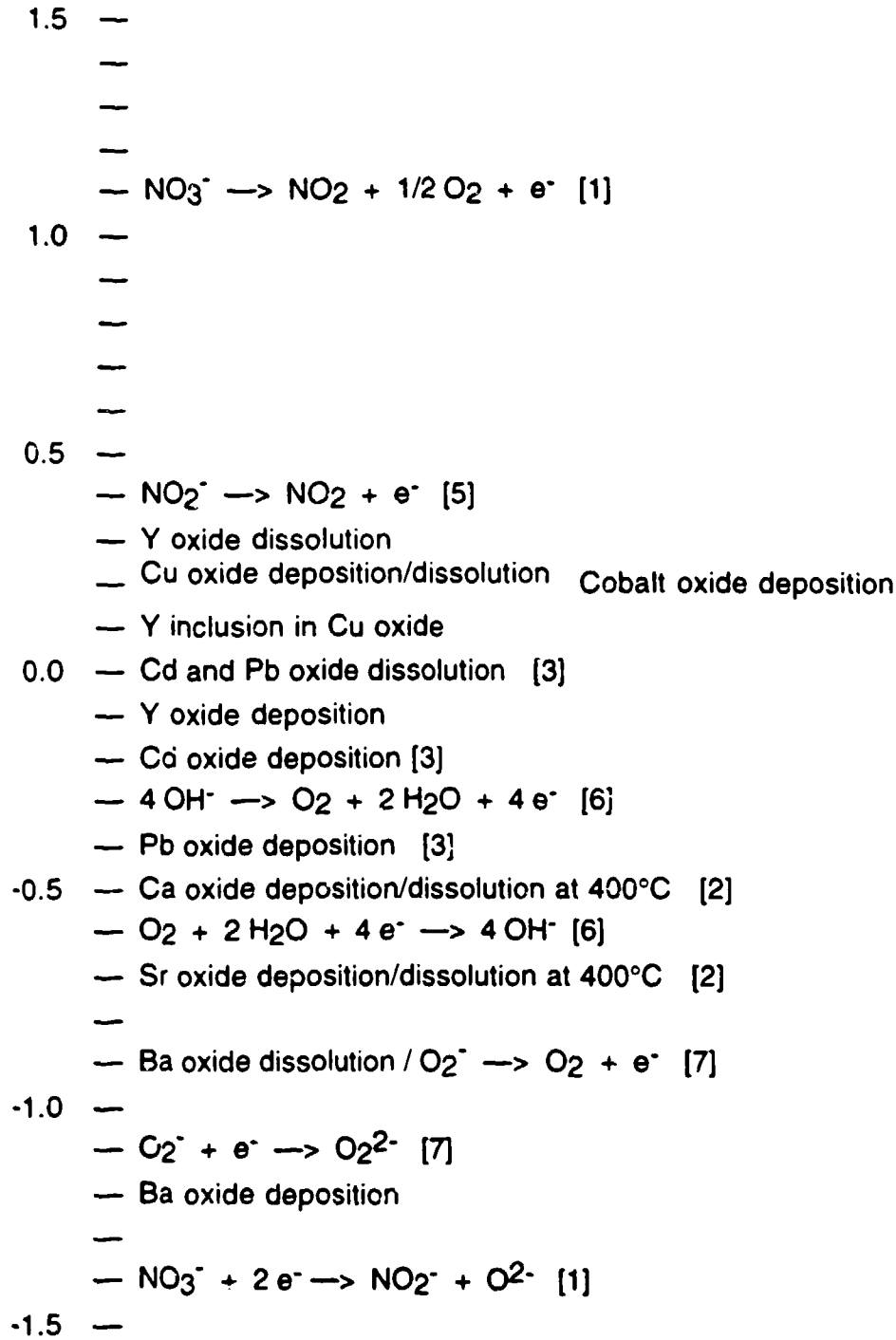

Fig. 2 Scale of onset potentials vs Ag/Ag^+ (0.07 M) for eutectic Na-K nitrate melt background reactions at 230°C, and metal oxide deposition processes at 300°C (this work) or 250°C (referenced work except [2]).

HTSC Deposition Experiments

Since all three Y-Ba-Cu components deposit as oxides from the molten nitrate system, a relatively straightforward approach was evaluated for deposition of HTSC material. A eutectic Ba-K nitrate melt (12.4 atom% Ba) was used to provide a large concentration of Ba^{2+} ions, and a Pt cathode was biased at potentials just positive of that required for Ba oxide deposition. In this case, Ba^{2+} will be included in the deposit only if underpotential deposition or compound formation occurs. To control the deposition sequence and amounts of Cu-Y oxides, which codeposit in this potential region, Cu^{2+} and Y^{3+} ions were injected as needed via electrodissolution of auxiliary Cu and Y anodes. A cell containing a small volume of melt was used to permit monolayer amounts of each oxide to be dissolved and redeposited on the anode in a short period of time. The Pt cathode was a wire that was rotated to provide melt mixing and more uniform deposition. The goal was to inject monolayer amounts of Cu^{2+} and Y^{3+} ions in the proper sequence so as to build up the oxide deposit a monolayer at a time. The occurrence of HTSC compound formation, which reduces the cathodic voltage required for deposition, would cause the Ba oxide to automatically be included in the deposit at the proper time and in the correct amount. This ion injection method could be viewed as the electrochemical analog of molecular beam epitaxy.

Figure 3 shows cyclic voltammograms for a Pt rotating disk electrode in the eutectic Ba-K nitrate melt at various temperatures (see appended papers for experimental details). At 315°C, the behavior is similar to that observed for the Na-K nitrate melt containing Ba^{2+} ions, except that the onset for Ba oxide deposition is more positive (-0.8 compared to -1.2 V) as would be expected for the higher Ba^{2+} concentration. At higher temperatures, increasing anodic and cathodic currents indicative of more facile melt decomposition are evident.

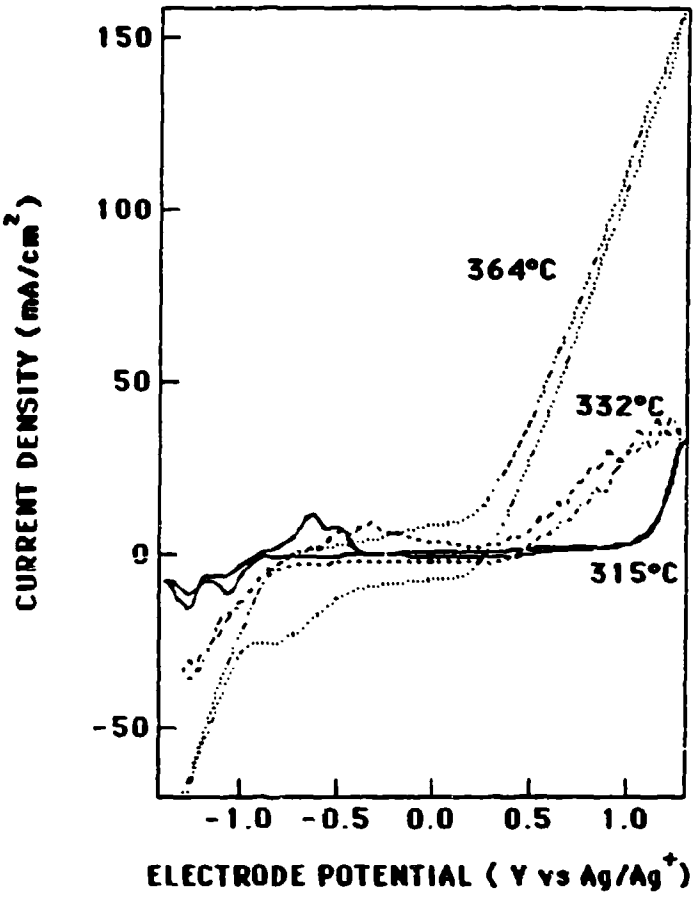

Fig. 3 Cyclic voltammograms (0.3 V/s) for a rotating Pt disk electrode (600 rpm) in eutectic Ba-K nitrate melt at various temperatures.

Figure 4 is a schematic representation of the cell used for the ion injection experiments. A small glass tube (7 mm i.d.) was fitted with two sidearms (for the auxiliary anodes) and a glass frit that allowed melt to be drawn into the cell from a reservoir contained in a glass beaker in the furnace well. The flat ground surface at the other end of the cell tube mounted to a stationary sleeve through which the rotating Pt cathode passed. The latter was a 1.6 mm diameter Pt wire attached via a set screw to a stainless steel rod and dipped into the melt to a depth 1.5 cm. The Pt counter electrode and Ag/Ag^+ reference electrodes were immersed in the reservoir melt (156 ml). The auxiliary anodes were approximately 1 mm diameter wires of OFHC Cu and ostensibly 99.9% Y (Johnson-Mathey, Reaction Grade, #12239, Lot # FM 336).

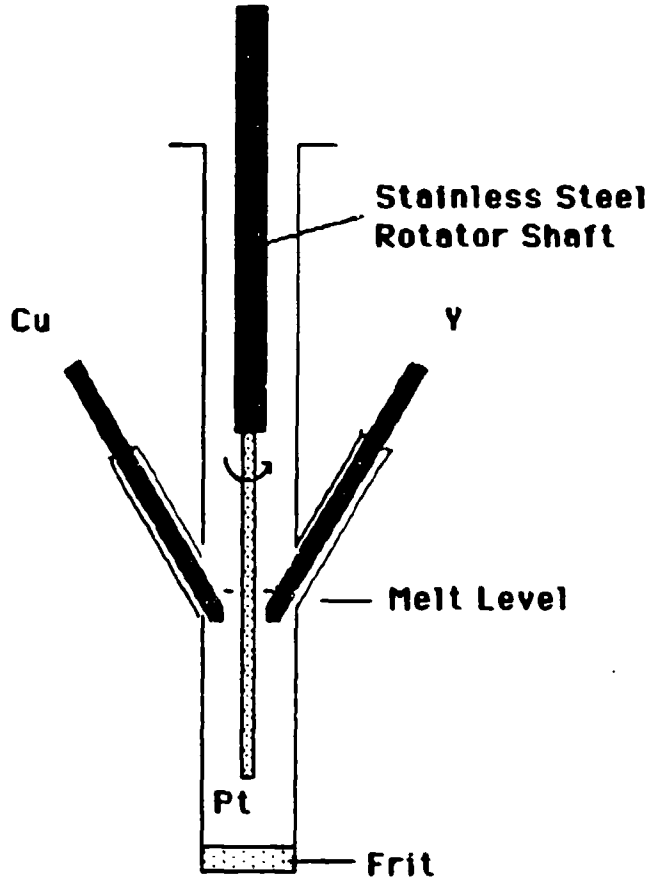

Fig. 4 Schematic representation of molten salt cell assembly used for mixed oxide deposition via sequential anodic injection of Cu^{2+} and Y^{3+} ions.

Figure 5 shows a schematic diagram of the system used maintain the rotating Pt wire cathode at constant potential and inject controlled amounts of Cu^{2+} and Y^{3+} ions into the melt. Galvanostatic pulses were obtained by applying a constant potential across a large series resistor (1 kohm) and the charge was determined by integrating the current. The injection pulses were always 12 and 24 mC for Cu and Y, respectively, and a delay of 10 s was allowed after each injection for deposition to occur. A computer was used to control the overall deposition process. The deposits obtained were analyzed by scanning electron microscopy (SEM), energy dispersive analysis of x-rays (EDAX) and x-ray diffraction.

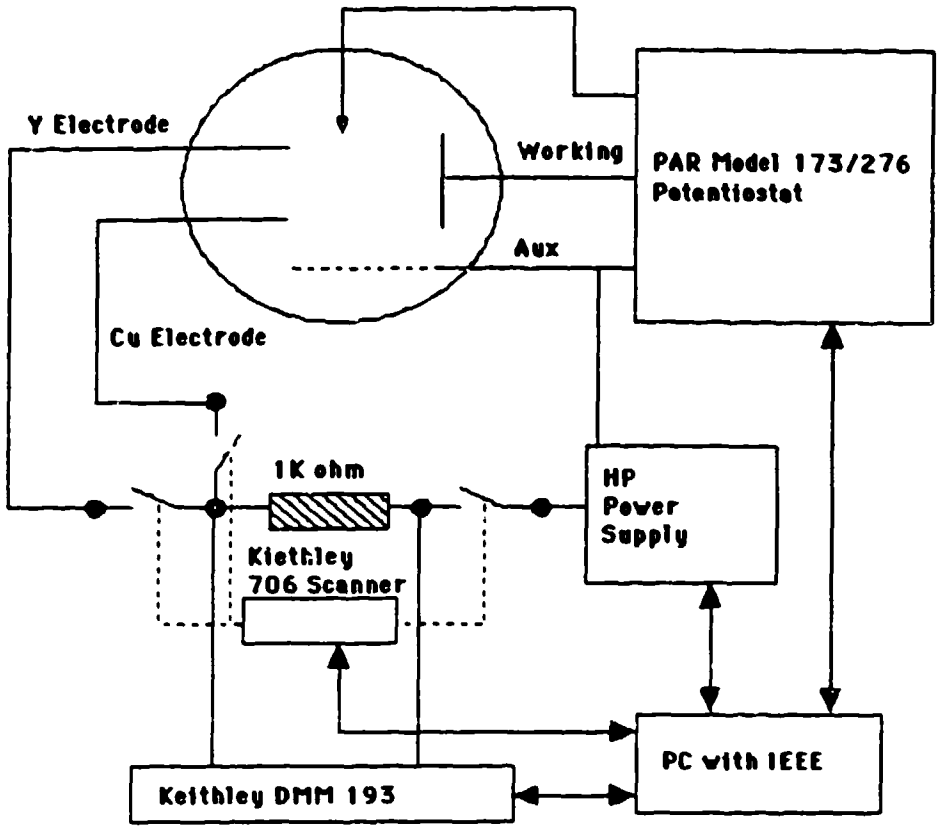

Fig. 5 Schematic block diagram of the system used for mixed oxide deposition via sequential anodic injection of Cu^{2+} and Y^{3+} ions.

Experiments were run at cathode voltages of -0.45, -0.625 and -0.8 V in a melt maintained at 332°C. At -0.45 V, the current was very small but 10 hours of injection deposition produced a black deposit that was poorly adhering and comprised of fine (10 μm diameter) nodules. At -0.625 V, the deposit obtained after 5.5 hours was very thick, comprised of an outer black layer that could be easily wiped away to expose a brown underlayer (also poorly adhering). After 6 hours at -0.8 V, the only deposit obtained was a dark band around the melt meniscus region. X-ray data indicated that all of the deposits were mostly amorphous, or comprised of exceedingly fine crystallites.

Table 1 summarizes the EDAX data for the deposits obtained by pulsed injection of Cu^{2+} and Y^{3+} ions. The most striking result is the inclusion of appreciable amounts (3.8 - 14.0 atom%) of Gd in the deposits. EDAX analysis of the wire used to inject Y^{3+} into the melt, which should have been 99.9% Y,

showed that the actual composition was 78 atom% Y and 22 atom% Gd. This is unfortunate since the deposits also contained mixed Ba-Y-Cu oxides (in various proportions), indicating that the injected ion approach has merit. Note that K was detected, indicating some occlusion of melt in the deposit specimens, but the Ba concentration increased with increased cathodic potential, suggesting that some Ba was included as part of mixed oxides. The composition of the band of deposit obtained at -0.8 V (29.6 atom% Cu, 16.6 Ba, 3.0 Y and 50.8 O) suggests that a mixed oxide containing all three metals is also deposited in this case but does not adhere to the Pt electrode except in the meniscus region (where the melt acidity may vary appreciably). Because of the Gd contamination, the results of these experiments is inconclusive. It is interesting to note that the Gd is enriched in the oxide compared to its concentration in the wire used for injection, an effect that might be optimized and exploited for materials separation.

Table 2
Composition (Atom%) of Deposits Obtained at Various Voltages

Voltage	Region	Ba	Cu	Y	Gd	K	O
-0.45	Region 1	0.5	19.1	13.8	7.8	4.5	54.3
-0.45	Region 2	0.2	30.9	8.4	4.4	3.9	52.2
-0.625	Top Layer	1.9	30.8	7.0	3.8	5.0	51.5
-0.625	Underlayer	2.2	8.7	12.0	14.0	8.8	54.3
-0.8	Dark Band	16.6	29.6	3.0	0	0	50.8

Future Work

These results show that cathodic deposition from nitrate melts is a very promising approach for preparing metallic oxides. However, it is recommended that future work initially focus on deposition of one- and two-component oxides, for which development of viable processes are inherently less complicated. The

two-component perovskite materials, which contain one electropositive metal and one with a large affinity for oxygen, are ideal candidates.

One of the key variables for mixed oxide deposition is temperature, which can enhance compound formation so as to improve the composition consistency of the deposit. Figure 6 shows the effect of temperature on cyclic voltammograms at a Pt electrode for a melt containing Cu^{2+} ion. There is little effect on the cathodic oxide deposition behavior, indicating that the molten nitrate melt provides considerable flexibility without respect to the operating temperature.

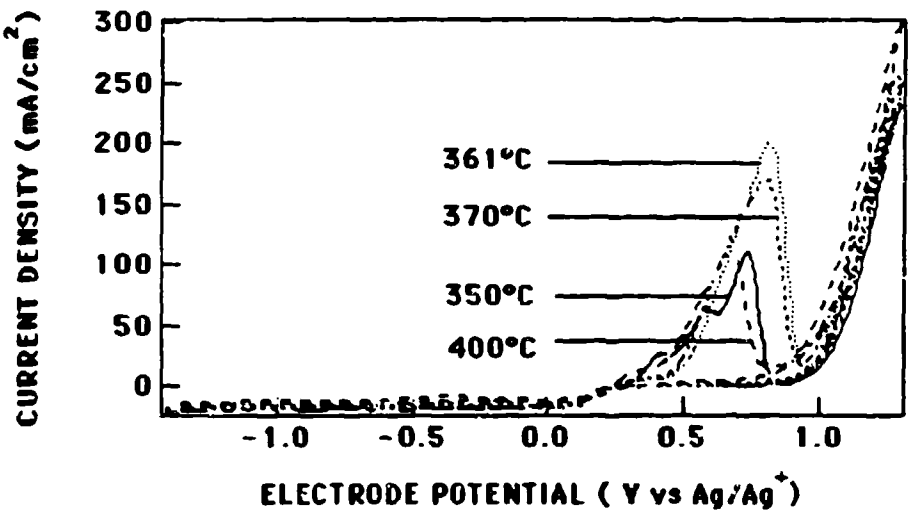

Fig. 6 Effect of temperature on cyclic voltammograms (0.3 V/s) for a rotating Pt disk electrode (600 rpm) in eutectic Na-K nitrate melt containing 10 mM Cu^{2+} ion.

REFERENCES

1. H. S. Swofford and H. A. Laitinen, J. Electrochem. Soc. 110, 814 (1963)

2. S. Stemberg and T. Visan, Electrochimica Acta 26,75 (1981)

3. M. H. Miles, Electrochemica Acta 32, 247(1987)

4. M. H. Miles, G. E. McManis and A. N. Fletcher, Proc. 5th Int. Symp. Molten Salts, ed. M. L. Sabcungi, K. Johnson, D. S. Newman and D. Inmen, Electrochem. Soc. Vol. 86-1, p. 234 (1986)

5. P. G. Zambonin and J. Jordan, J. Am. Chem. Soc. 89, 6365 (1967)

6. P. G. Zambonin, J. Electroanal. Chem. 33, 243 (1971); Anal. Chem. 43, 1571 (1971)

7. P. G. Zambonin and J. Jordan, J. Am. Chem. Soc. 91, 2225 (1969)

APPENDICES

Publications submitted to the Journal of the Electrochemical Society:

"Electrodeposition of Copper Oxide from the Eutectic Sodium-Potassium Nitrate Melt" by D. M. Tench, M. W. Kendig and S. Jeanjaquet

"Electrodeposition of Mixed Metal Oxide from the Eutectic Sodium-Potassium Nitrate Melt" by M. W. Kendig, D. M. Tench, S. Jeanjaquet and P. Stocker

Rockwell International
Science Center

SC71033.FR

Electrodeposition of Copper Oxide from the Eutectic Sodium-Potassium Nitrate Melt

D. M. Tench, M. W. Kendig and S. Jeanjaquet
Rockwell International Science Center
Thousand Oaks, CA 91360

ABSTRACT

Copper injected anodically into eutectic Na-K nitrate melt at 300°C is shown to deposit cathodically as the oxide (CuO). The dissolved copper is in the +2 oxidation state and apparently forms a nitrato complex that facilitates reduction of nitrate to oxide (and nitrite) at potentials more than a volt positive of that for reduction of the Na/K nitrate species. From these results and literature studies, cathodic metal oxide deposition from nitrate melts appears to be a general phenomenon that could prove to be a practical means of preparing anhydrous metal oxide films.

INTRODUCTION

Oxide films are of interest for a variety of practical applications, including corrosion protection, batteries, high temperature superconductors, catalysts, electronic devices, and flat panel displays. In many cases, anhydrous films are required but oxides produced by electrodeposition from aqueous electrolytes generally are at least partially hydrated. Dehydration can be effected by thermal treatments but the film quality attained is typically degraded because atomic/molecular rearrangements are involved. This is unfortunate since the electrodeposition approach is ideally suited to coating large areas and irregualar substrates, and can provide close control over the deposition process. One possibility for directly electrodepositing anhydrous metal oxides is to use a molten salt solvent.

Several studies have indicated the occurrence of direct cathodic deposition from nitrate melts of the oxides of a number of non-transition metals: K [1]; Ca, Sr and Ba [2]; Pb and Cd [3]; and Zn, In and Tl [4]. Since the observed reduction

potentials are up to a volt positive of the potential required for nitrate reduction in the background Na-K nitrate melt, metal oxide deposition probably occurs via a nitrato complex [3], i.e., according to:

$$(MONO_2)^+ + 2e^- \longrightarrow MO + NO_2^- \qquad (1)$$

for a divalent cation. Note that rapid nitrate reduction produced by high cathodic polarization in the pure Na-K nitrate melt results in deposition of sodium oxide, but the deposit eventually redissolves [1].

The present paper addresses the important practical question of whether transition metal oxides, specifically copper oxide, can also be deposited from nitrate melts. Previous workers [5-7] suggested that deposition of copper metal itself occurs, but they did not verify the nature of the deposits produced. In these earlier studies, Cu^{2+} was dissolved as either the nitrate (stabilized by addition of $KHSO_4$) or the chloride, and shown to introduce a diffusion-limited reduction wave (Pt electrode) with an onset at about +0.3 V vs Ag/Ag^+ [5,6]. Note that the onset voltage was identical whether Cu^{2+} was added as the chloride or nitrate, suggesting that the melt species might be the same in either case. Previous work [8,9] also indicates that Cu spontaneously forms Cu_2O in nitrate melts and that passivation, involving formation of CuO, occurs at about -0.1 V vs Ag/Ag^+ electrode.

EXPERIMENTAL DETAILS

Cell and Glove Box

Figure 1 depicts the molten salt electrochemical cell assembly used in the present work. The melt was contained in an open quartz beaker (6.3 cm dia.) inserted into a stainless steel well that was built into the floor of an argon-atmosphere glove box (Vacuum Atmospheres Corp., Los Angeles, CA) and was heated by an external furnace. The various electrode, thermocouple and gas feed-throughs were built into a water-cooled stainless steel lid that formed an o-ring seal with the glove box floor to permit control of the atmosphere within the furnace well (and cell). This cell compartment could be evacuated, or purged

with high-purity oxygen or argon that were passed over 13A molecular seives to ensure dryness. The temperature within the melt was monitored using a thermocouple sheathed in a pyrex tube and was controlled within 0.1°C by a Eurotherm proportional controller. The glove box atmosphere was continuously recirculated through a VAC Model 40-1 Dri-Train® gas purifier to maintain the partial pressures of water and oxygen below 1 and 10 ppm, respectively.

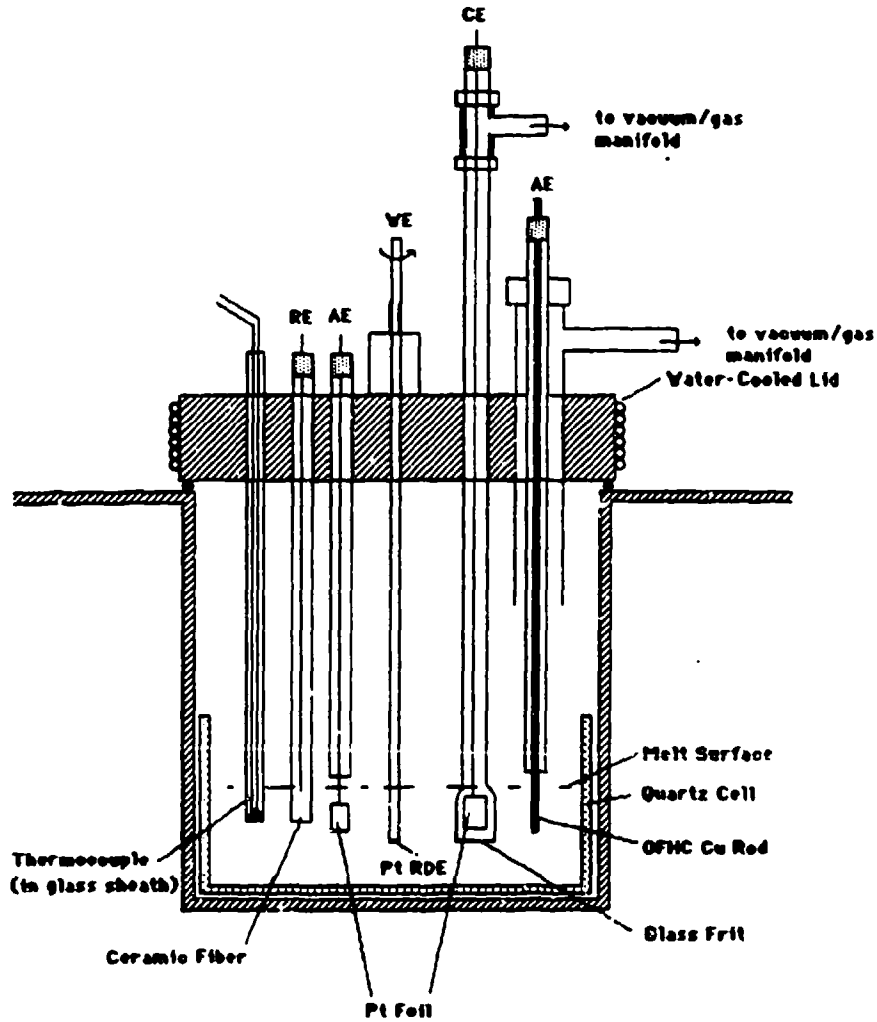

Fig. 1 Schematic representation of molten salt cell assembly, showing the reference (RE), rotating working (WE), counter (CE), and auxilliary (AE) electrodes.

Electrodes

In addition to the counter electrode, two auxilliary anodes were used: a Pt foil (6 cm^2) for melt purification; and an OFHC Cu rod (6.4 mm dia.) for injecting copper ions into the melt (see Fig. 1). To minimize contamination of the melt by species generated at the Pt foil counter electrode, the counter electrode compartment was isolated via a glass frit and was provided with a separate vent.

The Ag/Ag^+ reference electrode [10] was formed by immersing a 99.9% Ag wire (Wilkinson Co.) in a 0.07 M $AgNO_3$ solution in eutectic Na-K nitrate melt contained in a Pyrex glass tube. Electrical connection between the reference and main compartment melts was made via a porous ceramic (asbestos or zirconia) fiber sealed into the end of the glass reference compartment tube. The end of the tube external to the cell, through which the Ag wire passed, was sealed with epoxy. A small hole in the tube just below the cell lid served as a vent to ensure that there was no pressure differential between the reference and main compartments.

Figure 2 shows a schematic representation of the rotating Pt disk working electrode, which was fabricated by fusing the rim of a flint glass tube (0.7 cm diameter) to form a seal to a threaded Pt rod (0.63 cm diameter). The end of the electrode was ground flat and polished on successively finer aqueous alumina slurries to a 1 mm grit size. When heating and cooling were performed slowly, such electrodes were found to survive the thermal cycling associated with melt insertion and removal. However, comparable results were obtained using an unsheathed rotating Pt rod whose polished end was just touching the melt suface (position determined via electrical contact). In all cases, electrode rotation was provided by a Pine Instruments Model MSRX rotator/controller.

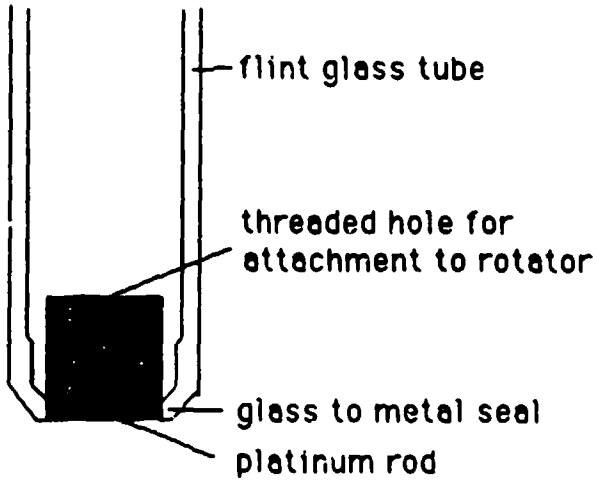

Fig. 2 Platinum rotating disk electrode construction.

Melt Purification

The eutectic melt was prepared by mixing high purity (99.999%) potassium nitrate and sodium nitrate salts (APL Engineered Materials, Urbana, IL) in the mass ratio of 1.188 (196.1 g KNO_3 and 165.0 g $NaNO_3$), and the mixture was dried under vacuum at 120-140°C for 16 hours. Fusion was performed under an atmosphere of dry oxygen to minimize reduction of nitrate to nitrite by carbonaceous impurities [11]. Vacuum pre-electrolysis at the Pt auxilliary electrode (1.05 V) was used to remove nitrite from the melt [11], presumably reducing its concentration to the value associated with nitrate dissociation, i.e., 2×10^{-4} molal [12]. Water was effectively removed simply by purging the melt with dry argon [13]. The melt temperature was always 300°C.

Instrumentation

Electrochemical measurements were made using a PAR Model 273 potentiostat under computer control with software supplied by PAR (Headstart©). The voltage sweep rate was typically 0.3 V/s, which yielded reproducible cyclic voltammograms. All data were stored on magnetic media for later analysis using graphics software provided by Wavemetrics (Igor©) and were digitally smoothed to reduce noise. Chronopotentiograms were recorded using a computer-controlled Keithley Model 199 scanning digital multimeter. Powder X-

ray diffraction measurements were made using a GE XRD5 with a Cu K_α source and solid state detector.

RESULTS AND DISCUSSION

Copper Melt Species

To avoid contamination of the melt by alternative anions or water of hydration from copper nitrate, Cu ions were introduced into the melt by electrochemical dissolution of an OFHC copper anode. Transpassive Cu dissolution has been reported to occur positive of 0.2 V in a two-electron process with 60-70% efficiency [9]. Based on this work, the melt species is apparently CuO_2^{2-} since evolution of NO_2 gas (formed by removal of oxygen from nitrate) was found to accompany anodic Cu dissolution.

In the present study, the oxidation state of Cu anodically injected into the melt was verified by measuring the charge associated with dissolution of a known quantity of Cu at constant voltage (1.05 V). The Cu had been electrodeposited on a Pt rod from an aqueous copper pyrophosphate bath (without organic additives) at 55°C, for which Cu deposition is a two-electron process with a current efficiency of 100%. As shown in Fig. 3, complete stripping of the Cu deposit was evident from a precipitous decrease in the current to the small background value.

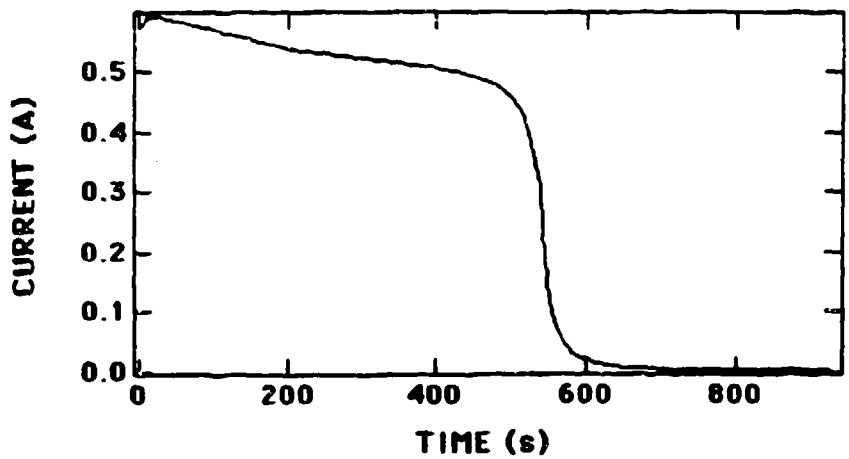

Fig. 3 Chronogalvanogram for the stripping of Cu at 1.05 V from a Pt substrate in eutectic Na-K nitrate at 300°C.

Table 1 compares the total charge (current x time) passed during Cu deposition from the pyrophosphate bath (Q_d) with that for stripping the deposit in the eutectic nitrate melt at 300°C (Q_s) for two experiments. In both cases, the stripping charge is comparable to the deposition charge, indicating that the Cu dissolution in the melt is also a two-electron process. The 10-14% lower Q_s values suggest that anodic Cu dissolution in the melt is only about 90% efficient. The Cu^{2+} melt concentrations specified below have been corrected for this inefficiency.

Table 1
Coulombs of Charge for Copper Aqueous Deposition (Q_d)
and Nitrate Melt Stripping (Q_s)

Q_d	Q_s	$(Q_d-Q_s)/Q_d$
324	291	0.10
957	826	0.14

Copper Oxide Deposition

Figure 4 shows cyclic voltammograms obtained at a Pt rotating disk electrode for the background melt and after injection of 10 and 30 mM Cu^{2+} ions. Anodic breakdown of the melt, which involves oxidation of nitrate to NO_2 and oxygen, is evident from the sharp current increase beginning at 1.1 V, whereas the cathodic limit (-1.4 V) is just short of cathodic melt breakdown [1]. This leaves a usable voltage range of 2.5 V over which the background current is generally less than 1 mA/cm^2, even with electrode rotation. The small cathodic wave beginning at -0.9 V apparently corresponds to reduction of superoxide, the predominant melt oxygen species, to peroxide [14]. This wave was variable in the present work, being usually smaller than in Fig. 4.

The salient features associated with Cu reactions are a cathodic wave (onset at 0.25 V) exhibiting a plateau from 0.0 V to melt breakdown, and a pronounced anodic peak at about 0.8 V. In addition, there is an anodic peak at about 0.0 V

(superimposed on the cathodic wave) and a small anodic wave beginning at 0.25 V, which are discussed below.

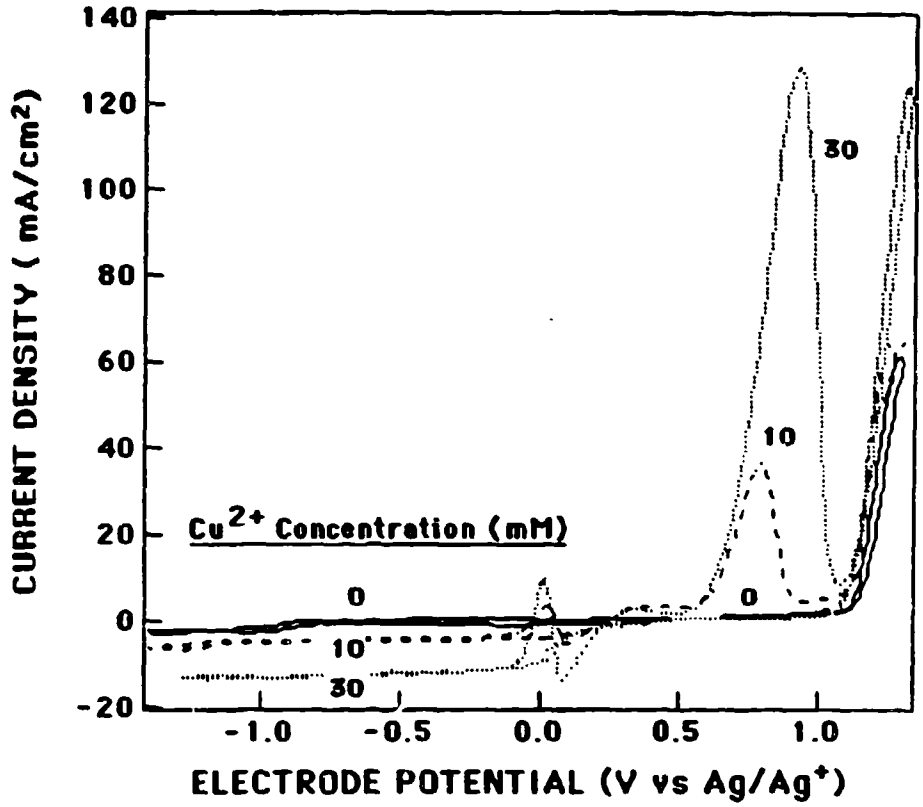

Fig. 4 Cyclic voltammograms (0.3 V/s) for a rotating Pt disk electrode (600 rpm) in background eutectic Na-K nitrate melt (300°C), and after addition of 10 and 30 mM Cu^{2+} ions.

Figure 5 shows Levich plots [15] of the reciprocal values of the cathodic plateau current associated with Cu^{2+} ion reduction and the square root of the electrode rotation rate. For both voltage sweep directions, the plots are linear at the higher rotation rates and pass through the orgin, indicating that the process associated with the cathodic wave is diffusion-limited. Note that deviations from linearity are expected for the lower rotation rates since the currents are relatively small so that interference from background currents is appreciable. The reciprocal slope of this plot (1/B) is given by:

$$1/B = 0.621\ n\ F\ C\ D^{2/3}\ \nu^{-1/6} \qquad (1)$$

where n is the number of electrons involved, F is Faraday's constant, C and D are the concentration and diffusion coefficient of Cu ions in the melt, w is the electrode rotation rate, and ν is the melt kinematic viscosity (viscosity divided by density). Assuming a two-electron process, $D \approx 3.1 \times 10^{-6}$ cm^2/s, based on a viscosity of 3.12 cp and a density of 1.909 g/cm^2 [16].

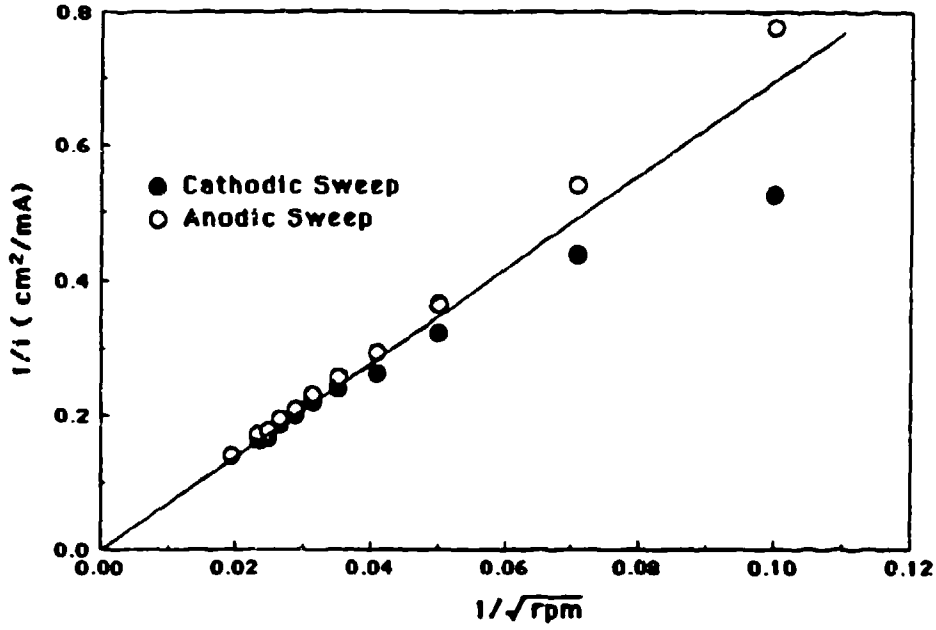

Fig. 5 Levich plots of the reciprocal cathodic current (i) at -0.6 V as a function of the reciprocal square root of the electrode rotation rate (rpm) for the anodic and cathodic scans at a Pt rotating disk electrode in a melt containing 10 mM Cu^{2+} ions.

By x-ray diffraction analysis of the deposit obtained at 0.0 V, the cathodic wave beginning at 0.4 V was shown to involve deposition of CuO. The deposition potential was chosen to be positive of the plateau region to avoid reactant diffusion limitations that can cause powdery deposits. Figure 6 shows a plot of the current density as a function of time during the deposition process. The current initially increases to a maximum after about 300 s and then decreases gradually, which is consistent with the deposition of a poorly conducting film. The deposit obtained was a smooth black film that gave the x-ray defraction

spectrum shown in Fig. 7, which indicates that it was composed predominantly of CuO (structure from the Pt substrate is also evident).

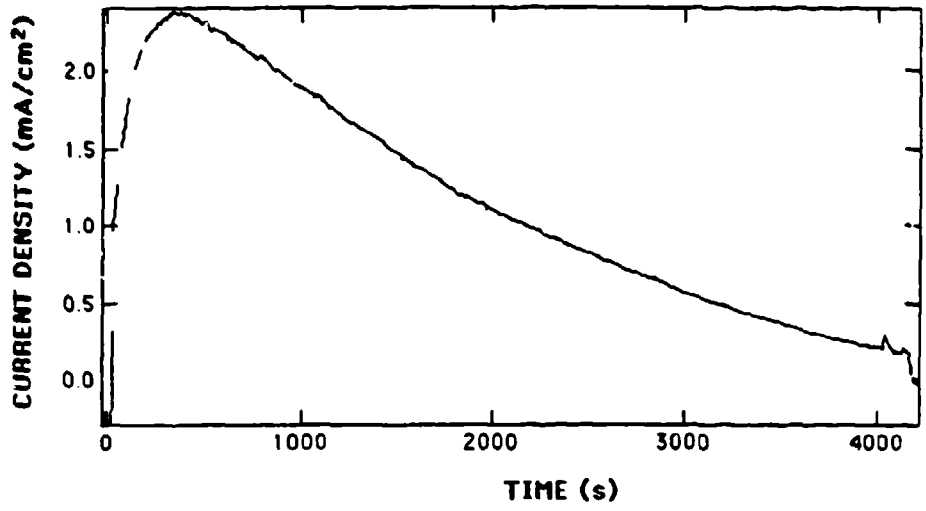

Fig. 6 Current as a function of time during deposition of CuO on a Pt rotating disk electrode (600 rpm) at 0.0 V in eutectic Na-K nitrate (300°C).

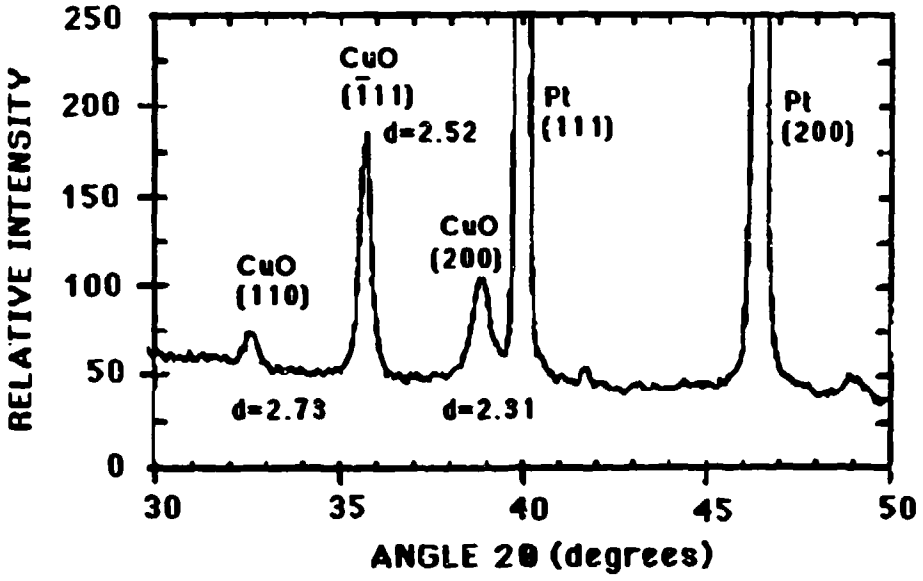

Fig. 7 X-ray diffraction scan of the deposit obtained under the conditions of Fig. 6.

Anodic Processes

Figure 8 shows cyclic voltammograms obtained for a melt with 30 mM Cu^{2+} ions at various cathodic sweep limits, with the region between -0.2 and 0.2 V shown with an expanded current scale (insert). Table 2 gives the integrated charges associated with the cathodic CuO deposition wave and the three anodic features. The large anodic peak at about 0.8 V reflects stripping of the CuO deposit from the Pt electrode since the corresponding integrated charge is approximately equivalent to that associated with the cathodic CuO deposition wave (considering both sweep directions). Note that the persistently larger value for the stripping charge is consistent with the anodic charge inefficiency observed for transpassive stripping of Cu metal deposits (Table 1). As expected, the anodic stripping peak (0.8 V) increases with electrode rotation rate (Fig. 9), but is independent of voltage sweep rate (Fig. 10). It should be mentioned that the cathodic deposition and anodic stripping charges do not correspond well for low melt Cu^{2+} concentrations (10 mM), presumably because background currents are relatively large in this case.

Table 2
Integrated Charge (mC/cm^2) for the
Voltammetric Features in Figure 8

Cathodic Wave (0.2 V)	Anodic Peak (0.8 V)	Anodic Peak (0.2 V)	Anodic Wave (0.2 V)	Total Anodic
105.3	101.1	5.4	1.7	108.2
82.6	87.6	6.5	1.5	95.6
72.9	77.4	4.4	1.3	83.1
62.7	63.3	1.4	1.2	65.9
45.1	47.3	0.0	1.5	48.7

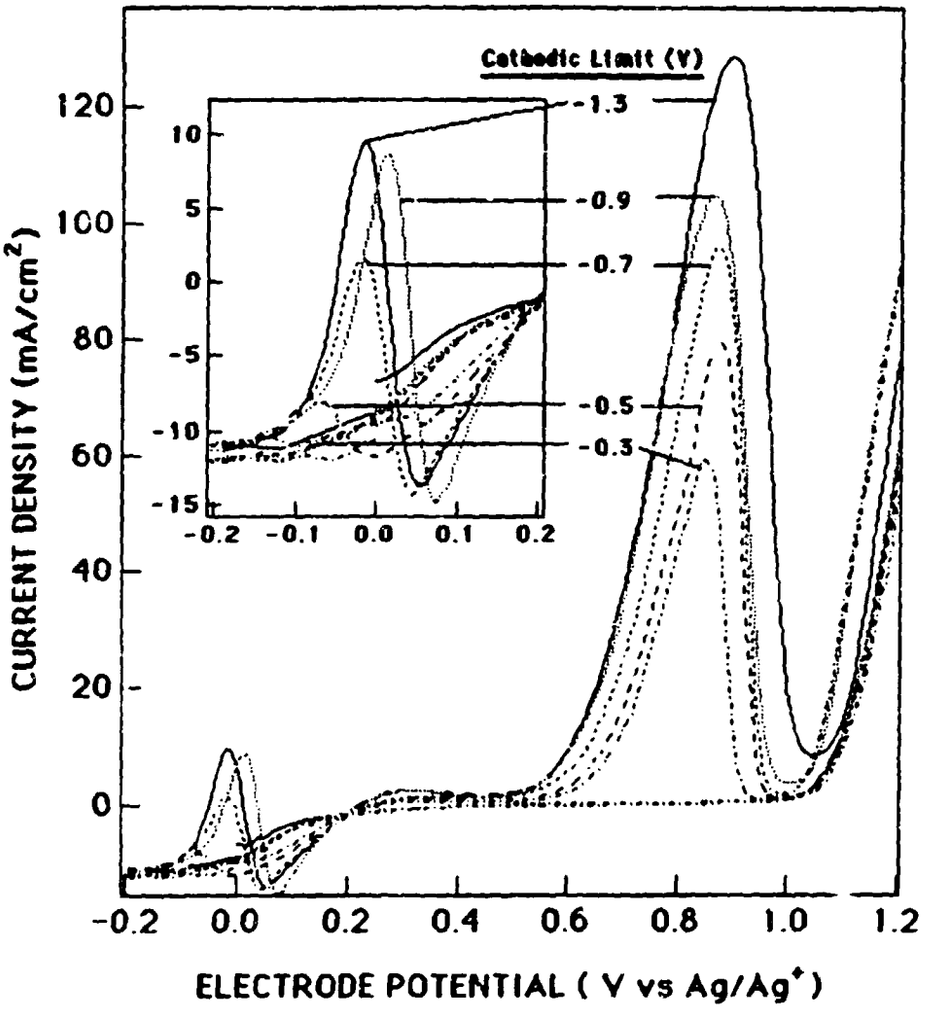

Fig. 8 Effect of cathodic sweep limit on the cyclic voltammetric behavior (0.3 V/s) of a Pt rotating disk electrode (600 rpm) in eutectic Na-K nitrate melt (300°C) containing 30 mM Cu^{2+} ions.

THIS
PAGE
IS
MISSING
IN
ORIGINAL
DOCUMENT

28

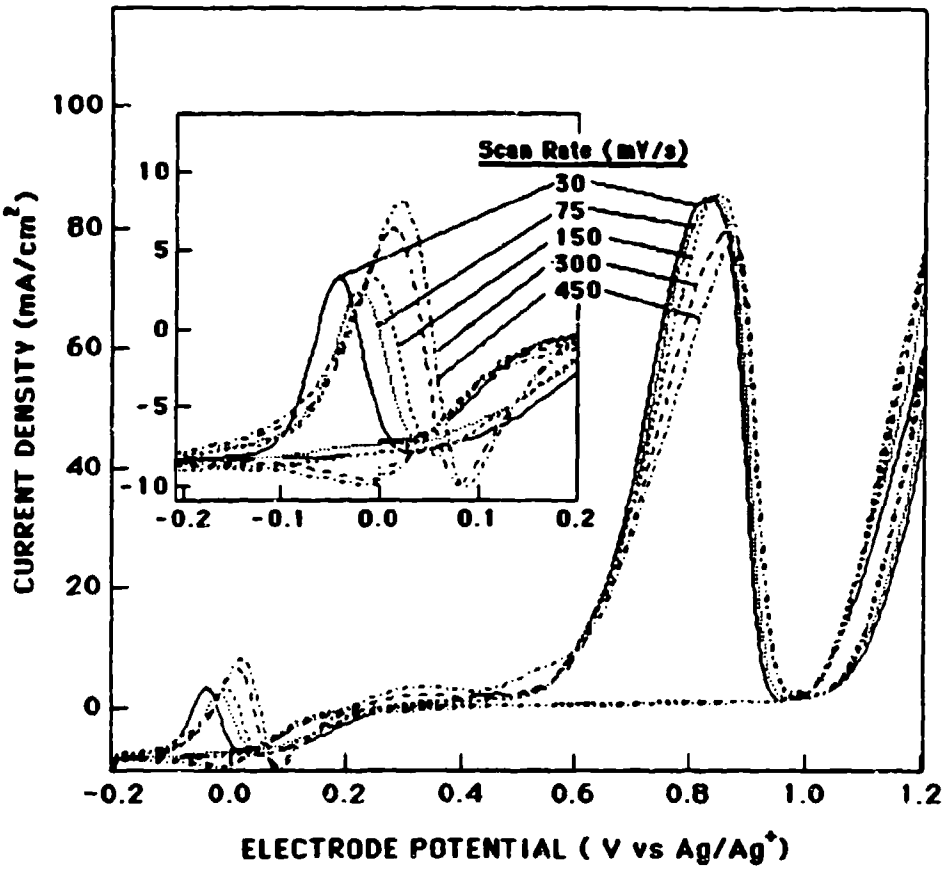

Fig.10 Effect of voltage scan rate on the cyclic voltammetric behavior (between -0.9 and 1.2 V) of a Pt rotating disk electrode (600 rpm) in eutectic Na-K nitrate melt (300°C) containing 30 mM Cu^{2+} ions.

The small anodic peak superimposed on the cathodic CuO deposition wave and occurring at about 0.0 V presents a puzzle. It is enhanced by electrode rotation and is evident only for rotation rates above 200 rpm (Fig. 9), suggesting that reaction with a melt species in relatively low concentration is involved. If we assume a somewhat reasonable surface roughness factor for the deposit of 10, the maximum integrated peak area of about 5 mC/cm² (Table 2) is consistent with a reactant surface coverage in the monolayer region. However, the peak appears only when the cathodic sweep limit is negative of -0.3 V (Fig. 8), indicating that a simple surface reaction is not responsible. Note that deposition of some Cu species, presumably CuO, continues during the anodic sweep and

would tend to cover an interfacial species formed at more cathodic potentials before the potential of the anodic peak (0.0 V) were reached. Apparently, some melt species is adsorbed at the interface but manages to avoid being incorporated in the deposit by desorption and re-adsorption as the deposit grows.

The species responsible for the anodic peak at 0.0 V may be related to that associated with the anodic wave beginning at 0.25 V since the latter is diminished when the former is enhanced (see Figs. 8 and 9). Nitrite is known to undergo electrochemical oxidation to nitric oxide (NO_2) at about 0.4 V on Pt electrodes [17], suggesting that this process may be responsible for the anodic wave observed in our work. Since a shift in the potential for nitrite oxidation on a copper oxide surface is likely, the anodic peak at 0.0 V might correspond to oxidation of some adsorbed nitrite species.

Anodic dissolution of the CuO deposit would be expected to occur by reaction with either nitrate:

$$CuO + ONO_2^- \rightarrow Cu(ONO_2)^+ + 1/2\ O_2 + 2\ e^- \qquad (2)$$

or residual nitrite ion:

$$CuO + ONO^- \rightarrow Cu(ONO_3)^+ + 2\ e^- \qquad (3)$$

Since the former should depend on the oxygen partial pressure but saturating the melt with oxygen instead of argon was found to have no effect on any of the voltammetric features, reaction (3), involving nitrite, seems likely. This is also consistent with the observation that the anodic voltammetric features tend to be somewhat irreproducible from run to run, as would be expected if a reactant is present in low (and somewhat variable) concentration. Stripping of the CuO deposit at more negative potentials may be limited by slow desorption of adsorbed $Cu(ONO_3)^+$ species, which would be more readily desorbed as the electrode potential is increased, particularly positive of the point of zero charge.

CONCLUSIONS

Copper oxide (CuO) is cathodically deposited from eutectic Na-K nitrate melt (300°C) at potentials negative of 0.25 V vs Ag/Ag^+ (0.07 M), more than a volt positive of the melt breakdown potential. Deposition apparently occurs via reduction of nitrate in a copper nitrato complex, as previously suggested for non-transition metals [1-4]. Anodic stripping of CuO deposits is a complicated process that is apparently inhibited by adsorption of nitrite, rapid dissolution occurring only a potentials positive of 0.6 V.

There are important differences between depostion of metal oxides from nitrate melts and the seemingly analogous cathodic deposition of metal hydroxides from aqueous solutions. In addition to the obvious difference that no protons are involved, oxide deposition proceeds via direct reduction of a metal nitrato complex. Cathodic hydroxide deposition, on the other hand, involves water reduction to form the hydroxide, which precipitates the solvated metal ion. Consequentially, there is virtually no change in the overvoltage for cathodic formation of hydroxide upon introduction of the metallic ions. The large shift in potential associated with oxide deposition from a nitrato complex offers new opportunities for deposition of both single and mixed metal oxides.

ACKNOWLEDGEMENT

This work was performed under DARPA Contract No. N00014-90-C-0225, which was administered by the Office of Naval Research.

REFERENCES

1. H. S. Swofford and H. A. Laitinen, J. Electrochem. Soc. 110, 814 (1963)

2. S. Sternberg and T. Visan, Electrochim. Acta 26, 75 (1981)

3. M. H. Miles, Electrochemica Acta 32, 247 (1987)

4. M. H. Miles, G. E. McManis and A. N. Fletcher, Proc. 5th Int. Symp. Molten Salts, ed. M. L. Saboungi, K. Johnson, D. S. Newman and D. Inmen, Electrochem. Soc. Vol. 86-1, p. 234 (1986)

5. I. D. Panchenko and G. V. Shilina, J. Anal. Chem. (USSR) 18, 799 (1963)

6. G. Mamantov, J. M. Strong and F. R. Clayton, Jr., Anal. Chem. 40 (3), 488 (1968)

7. D. G. Winter and P. J. Bowles, Adv. Extr. Met. Refining, Proc. Int. Symp., Jones, ed., Inst. Mining Met., London, 437 (1972)

8. A. Conte, Electrochim. Acta 11, 1579 (1966)

9. T. Notoya, Denki Kagaku 41, 779 (1973)

10. L. G. Boxall and K. E. Johnson, Anal. Chem. 40, 831 (1968)

11. H. S. Swofford, Jr. and P. G. McCormick, Anal. Chem. 37, 970 (1965)

12. R. N. Kust and J. D. Burke, Inorg. Nucl. Chem. Lett. 6, 333 (1970)

13. P. G. Zambonin, J. Electroanal. Chem. 33, 243 (1971)

14. P. G. Zambonin and J. Jordan, J. Am. Chem. Soc. 91, 2225 (1969)

15. V. G. Levich, Physicochemical Hydrodynamics, Prentice-Hall, Englewood Cliffs, N. J., 1962

16. I. G. Murgulescu and S. Zuca, Electrochem. Acta 14, 519 (1969)

17. P. G. Zambonin and J. Jordan, J. Am. Chem. Soc. 89, 6365 (1967)

Electrodeposition of Mixed Metal Oxides from the Eutectic Sodium-Potassium Nitrate Melt

M. W. Kendig, D. M. Tench, S. Jeanjaquet and P. Stocker
Rockwell International Science Center
1049 Camino dos Rios
Thousand Oaks, CA 91360

ABSTRACT

Mixed yttrium-barium-copper oxides have been deposited cathodically on CuO/Cu substrates from eutectic Na-K nitrate melts (300°C) containing dissolved Y^{3+} and Ba^{2+} nitrate species. Cobalt oxide has also been deposited from this system by cathodic reduction of Co^{2+} nitrate ions at a Pt electrode. Available data for Na-K nitrate melts have been summarized to facilitate the design of schemes for deposition of various mixed metallic oxides.

INTRODUCTION

Work in several laboratories has indicated that the oxides of non-transition metals, i.e., K [1], Ca, Sr and Ba [2], Pb and Cd [3], and Zn, In and Tl [4,5], rather than the free metals, are cathodically deposited from nitrate melts. As suggested by Miles et al. [3-5], the oxides are apparently deposited from metal-nitrate complexes since the deposition potentials are sometimes very positive of the melt breakdown potential. Recently, we have demonstrated that cathodic oxide deposition indeed occurs and also obtains for transition metals [6], indicating that it is a general phenomenon. In the case of copper, the deposit was shown to be CuO by x-ray diffraction analysis. The present work addresses some of the key considerations in developing viable processes for deposition of mixed metal oxides from nitrate melts. Emphasis is on providing the basis for deposition of the Y-Ba-Cu oxides that are currently receiving intense attention because of their high-temperature superconducting properties. Deposition of perovskite materials is also considered.

Approach Rationale

The major problem in manufacturing practical high-temperature superconductor (HTSC) oxide films is that low-temperature processing is needed for most practical applications but methods investigated to date do not yield materials of sufficient quality, even with the use of high-temperature sintering operations. Direct electrodeposition of the superconducting oxide itself from a molten salt in which the component species are dissolved would provide considerable benefit. Solid-state reactions and diffusional processes that invariably lead to high concentrations of defects and grain boundaries are avoided, and processing temperatures in the 200-600°C range are possible. In situ preparation allows exploitation of favorable reaction free energies to permit formation of ordered HTSC structures at the lowest possible temperature. Electrodeposition enables the addition of more energy in small increments and thus should further reduce the temperature required and provide precise control over the deposition process. This method is also applicable to irregular-shaped substrates and direct pattern deposition, and is readily scaled up or down.

One subtle but important feature of electrodeposition processes is a pronounced tendency toward formation of strong texture and large grains even on mismatched or disordered substrates. This is a consequence of the near-equilibrium deposition conditions attainable via electrical control, as opposed to thermal activation for which the depositing species typically arrive at the surface with considerable excess energy.

Pertinent Nitrate Melt Chemistry

The present good understanding of oxygen species in eutectic Na-K nitrate melts is due primarily to Zambonin and coworkers, who showed that the predominant species in the anhydrous system (at 250°C) is superoxide (O_2^-) [7-11]. The oxide (O^{2-}) and peroxide (O_2^{2-}) species are spontaneously oxidized by nitrate to superoxide according to:

$$O^{2-} + NO_3^- = O_2^{2-} + NO_2^- \quad (1)$$

$$O_2^{2-} + 2\,NO_3^- = 2\,O_2^- + 2\,NO_2^- \quad (2)$$

The equilibrium for reaction (1) lies far to the right so that only superoxide and peroxide are thermodynamically stable, and the latter is converted quantitatively to superoxide in the presence of oxygen via:

$$O_2^{2-} + O_2 = 2\,O_2^- \qquad (3)$$

This picture is supported by extensive electrochemical data [7-11], electron paramagnetic resonance detection of superoxide [12], independent manometric measurements of the oxygen uptake associated with reaction (3) above [13], and good correlations with similar solid-state data [14].

Zambonin [15] also showed that water quantitatively converts superoxide to hydroxide (OH^-) within a few hours:

$$2\,O_2^- + H_2O = 3/2\,O_2 + 2\,OH^- \qquad (4)$$

This, of course, introduces additional electrochemical reactions that would have to be taken into account in wet melts.

EXPERIMENTAL DETAILS

Apparatus and Procedures

The argon-atmosphere glove box, controlled-atmosphere furnace well/glass cell, and procedures used in the present work were the same as those described previously [6]. The eutectic Na-K nitrate melt was operated at 300°C and was pre-electrolyzed at a Pt anode to remove residual nitrite remaining after the reagents had been fused under an oxygen atmosphere. All electrode potentials are given relative to the $Ag/AgNO_3$ (0.07 M) reference electrode [16].

Except for Ba, electroactive metal ions were injected into the melt by anodic dissolution of the high-purity metals, i.e., 99.9% Y foil (Johnson-Matthey), 99.9% Co foil (Atomergics), and OFHC Cu rod. Actual concentrations were verified by

atomic absorption analysis of melt samples. Barium ions were introduced into the melt by dissolution of reagent grade barium oxide (BaO).

Auger electron spectroscopy (AES) data were obtained using a Phi 590 spectrometer. Peak to peak heights for differentiated spectra were scaled using the relative elemental sensitivities [17] to provide atomic percents for the various surface species. Depth profiling was performed via argon ion sputtering.

Working Electrodes

Cyclic voltammetric experiments were performed using the Pt rotating disk electrode described previously [6]. Copper working electrodes used for deposition of mixed oxides were cut from 3-mm thick OFHC Cu sheet and had an exposed area of 4 cm^2 (both sides). They were etched in 25% nitric acid, rinsed in deionized water, and dried before being transfered into the glove box.

RESULTS AND DISCUSSION

Yttrium Electrochemistry

As shown by the cyclic voltammograms in Fig. 1, Y metal is very active in the nitrate melt. Anodic current corresponding to Y dissolution is evident beginning at about -1.0 V, just 0.4 V positive of the potential for cathodic melt breakdown (-1.4 V) at Pt electrodes. The relatively slow rise in current and the plateau observed during the faster anodic voltage scan suggent that the dissolution process is kinetically inhibited. It is also significant that the onset potential for cathodic melt breakdown on the Y surface is shifted (compared to that on Pt) by -0.5 V (to -1.9 V). This indicates that adsorption of metal nitrato complexes on Pt probably plays an important role in nitrate reduction processes.

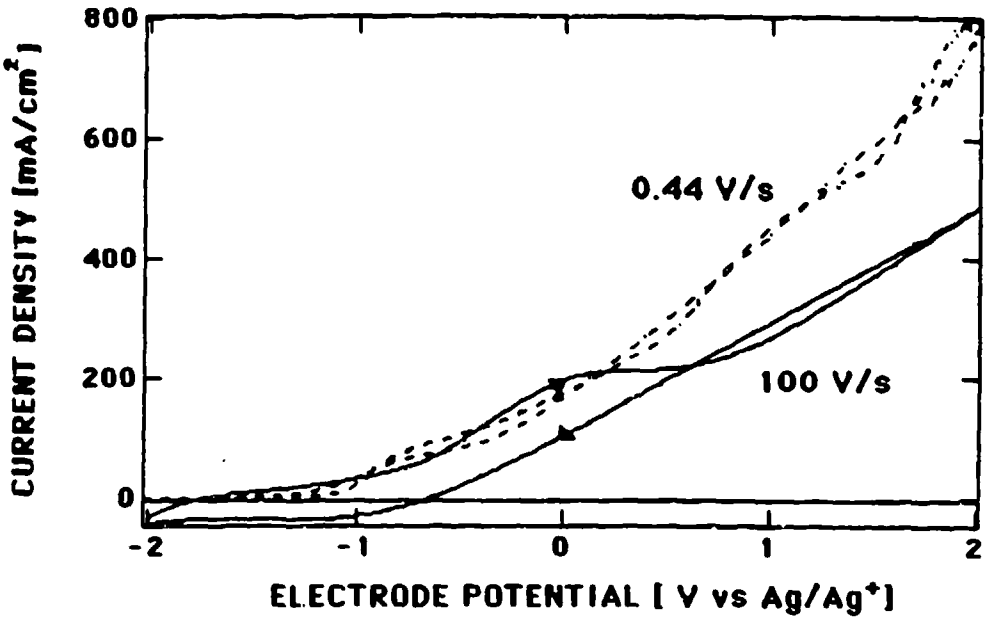

Fig. 1 Cyclic voltammograms at 0.44 and 100 V/s for a stationary Y foil electrode in eutectic Na-K nitrate melt at 300°C.

Figure 2 illustrates the voltammetric behavior of a rotating Pt electrode in a melt containing 30 mM Y^{3+} ion. As was previously found to be the case for Cu^{2+} ion [6], a mass transport limited cathodic wave, presumably corresponding to deposition of yttrium oxide (Y_2O_3), and an anodic stripping peak are apparent. Films obtained on Pt electrodes from yttrium-containing melts were not analyzed but Y_2O_3 was shown by AES analysis to deposit on CuO/Cu substrates, as discussed below. The onset potential for deposition of Y_2O_3 on Pt (-0.1 V) is -0.35 V negative of that for CuO deposition (0.25 V). As indicated by the relatively high current after the stripping peak (Fig. 2), Y_2O_3 stripping apparently continues into the anodic melt breakdown region (at the voltage scan rates investigated) so that deposition and stripping charges could not be meaningfully compared.

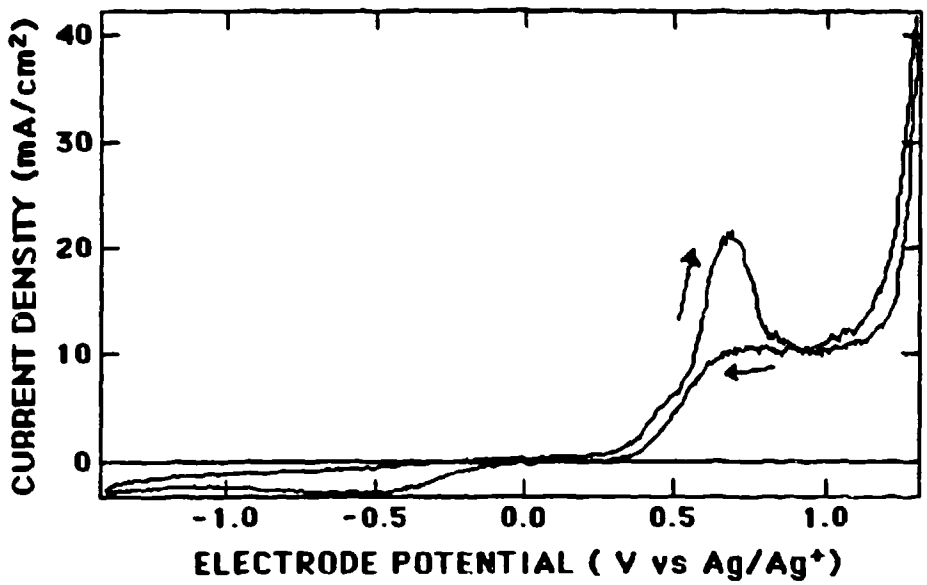

Fig. 2 Cyclic voltammograms (0.3 V/s) for a Pt rotating disk electrode (600 rpm) in eutectic Na-K nitrate melt (300° C, containing 30 mM in Y^{3+} ion.

Barium Ion Electrochemistry

Figure 3 shows cyclic voltammograms at a rotating Pt electrode in melts containing Ba^{2+} alone, and Ba^{2+} and Cu^{2+} ions together. In contrast to Cu^{2+} and Y^{3+}, the onset potential for Ba^{2+} reduction is very negative (-1.2 V), occurring very near to the melt breakdown potential (-1.4 V). The species deposited is presumably BaO but this was not verified since the highly reactive metal, if formed, would undoubtedly oxidize upon exposure to air, rendering x-ray analysis results ambiguous. Stripping of the Ba-based deposit in the absence of Cu^{2+} ions produces a well-defined peak at -0.4 V (Fig. 3) and, as is also the case for Cu and Y oxides, the overvoltage separating the deposition and stripping processes is appreciable (about 0.3 V). Note that this would be unlikely if the deposit were Ba metal, which is highly reactive.

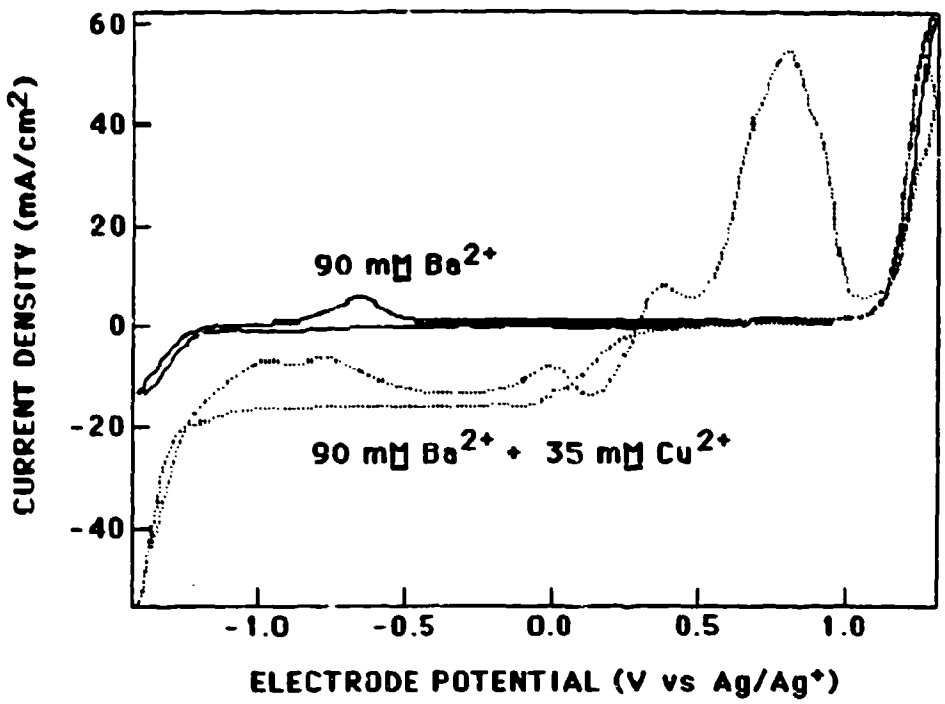

Fig. 3 Cyclic voltammograms (0.3 V/s) for a roatiting Pt disk electrode (600 rpm) in eutectic Na-K nitrate melt (300°C) containing 90 mM Ba^{2+} alone, or 90 mM Ba^{2+} plus 35 mM Cu^{2+} ion.

For the melt that also contained Cu^{2+} ion (Fig. 3), the voltammogram is identical to that obtained for Cu^{2+} alone [6], except for the barium oxide deposition/stripping currents superimposed on the CuO deposition wave at potentials negative of -0.4 V. On the other hand, stripping of the barium-based deposit occurs over a broader potential range in the presence of Cu^{2+} ion, presumably reflecting codeposition of copper oxide.

Individual Metal Ion Behavior

Figure 4 compares cyclic voltammograms at a Pt rotating electrode for melts containing either Cu^{2+}, Y^{3+} or Ba^{2+} ions. It is evident that in the absence of the other ions, deposition of Cu oxide would occur first on the Pt surface, then Y oxide, and finally the Ba species as the potential is decreased. Also, because of the overvoltage associated with stripping of the Y oxide deposit, deposition of an overlayer of CuO in the absence of other deposition processes would

appear to be possible between 0.25 and -0.1 V. Likewise, codeposition of Cu and Y oxides in the absence of deposition of a Ba species appears possible between -0.1 and -1.2 V. However, it should be kept in mind that for deposition of one material upon another or for codeposition, underpotential deposition and/or compound formation is likely to alter this picture considerably.

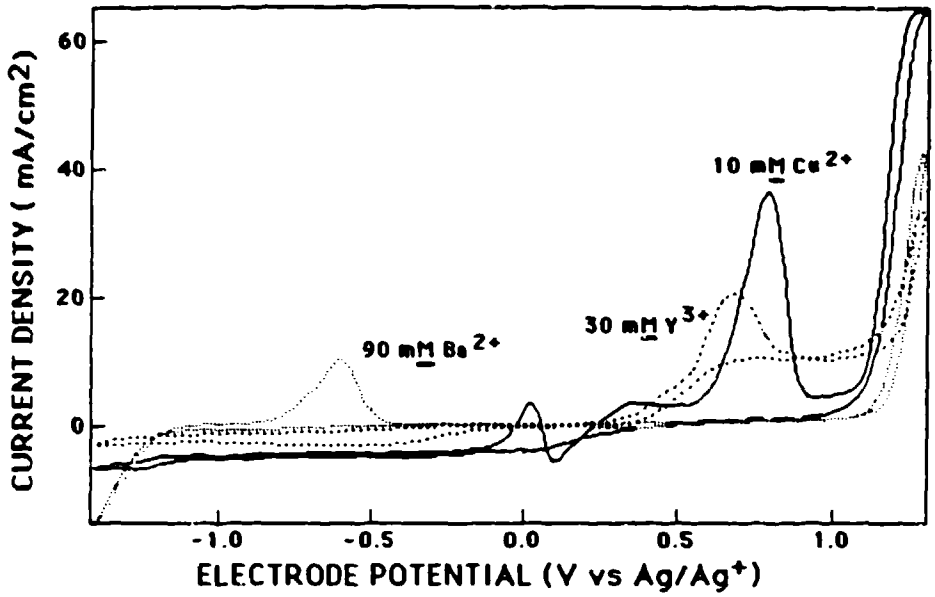

Fig. 4 Cyclic voltammograms (0.3 V/s) for a roatiting Pt disk electrode (600 rpm) in eutectic Na-K nitrate melt (300°C) containing either 30 mM Y^{3+}, 10 mM Cu^{2+} or 90 mM Ba^{2+} ion.

Mixed Yttrium-Copper Oxides

As the first step in depositing mixed metal oxides, Cu electrodes, which are covered with a surface oxide over most of the accessible potential range [18,19], were biased at various voltages for five minutes in a melt containing 30 mM Y^{3+} ion. In some experiments, one minute was allowed for formation of the natural melt oxide, whereas in other experiments the electrode was introduced into the melt with the voltage applied. Current transients at various bias voltages are shown in Figs. 5 and 6, respectively. In both cases, the overall current is anodic at potentials positive of 0.2 V, apparently reflecting dissolution of the Cu electrode, and cathodic at negative voltages, reflecting deposition of an Y species. The steady-state cathodic current is practically independent of the

applied voltage, which would be expected for a diffusion-controlled deposition process. There are two features observed in the current transients for the equilibrated Cu electrode (Fig. 5), but not when the electrode is inserted with the voltage applied (Fig. 6) or in the absence of Y^{3+} in the melt [6], that indicate formation of a mixed Cu-Y oxide on open circuit. The first is the initial cathodic peak which indicates that deposition of Y^{3+} from the melt is more facile on the equilibrated Cu surface. The second feature is the anodic current fluctuations observed after the initial anodic peak (Fig. 5), indicative of breakdown and reformation of the surface oxide as Cu dissolves anodically.

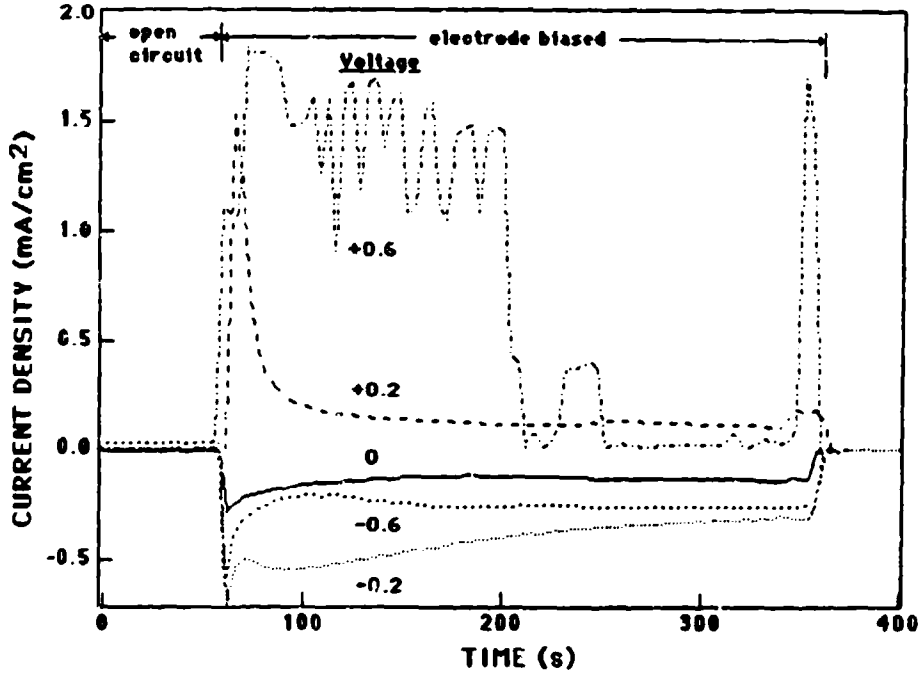

Fig. 5 Current as a function of time for stationary Cu electrodes biased at various potentials after one minute on open circuit in eutectic Na-K nitrate melt (300°C) containing 30 mM Y^{3+} ion.

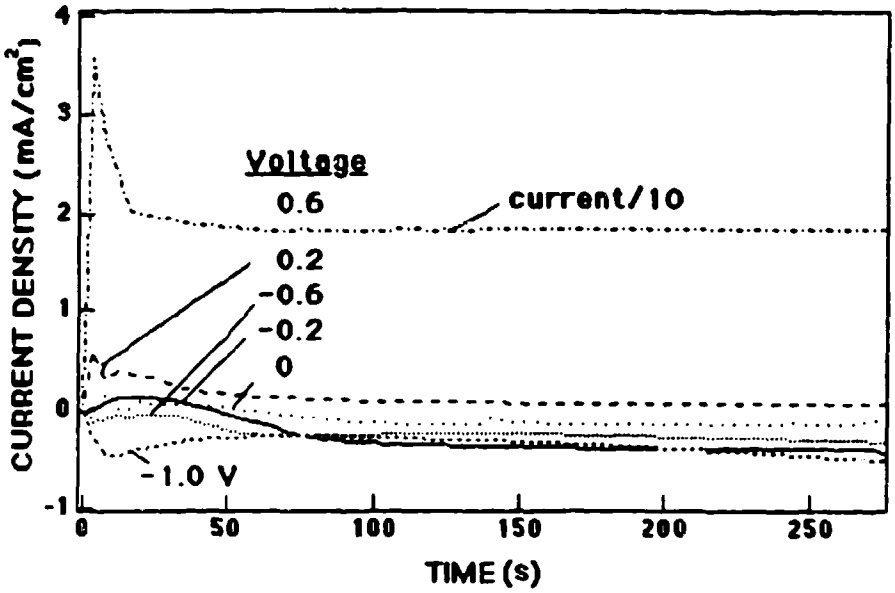

Fig. 6 Current as a function of time for stationary Cu electrodes introduced with various potentials applied into eutectic Na-K nitrate melt (300°C) containing 30 mM Y^{3+} ion.

Figure 7 shows the potential dependence of the atomic percent Cu, Y and O detected by AES for Cu electrodes equilibrated for one minute before the voltage was applied. For potentials positive of about 0.2 V, for which the overall current is always anodic, only Cu and O in the atomic ratio of 1:1 are detected, indicating that the surface of the dissolving Cu electrode is covered with CuO. However, at negative potentials, a mixed Cu-Y surface oxide is formed for which the Cu content decreases to a minimum at about -0.2 V and then increases, which is somewhat surprising since Y oxide deposition occurs on Pt in this potential range. Apparently, direct deposition of ytterium oxide is inhibited on the CuO surface compared to formation of mixed Cu-Y oxide. Formation of a mixed Cu-Y oxide is also evident from the AES depth profile in Fig. 8 for an equilibrated Cu electrode that had been biased at -0.2 V. Over a depth of 2000 Å, the composition is constant at 63% O, 33% Y and 4% Cu, corresponding to a mixed oxide having a nominal composition of $Cu_{0.2}Y_{1.8}O_3$.

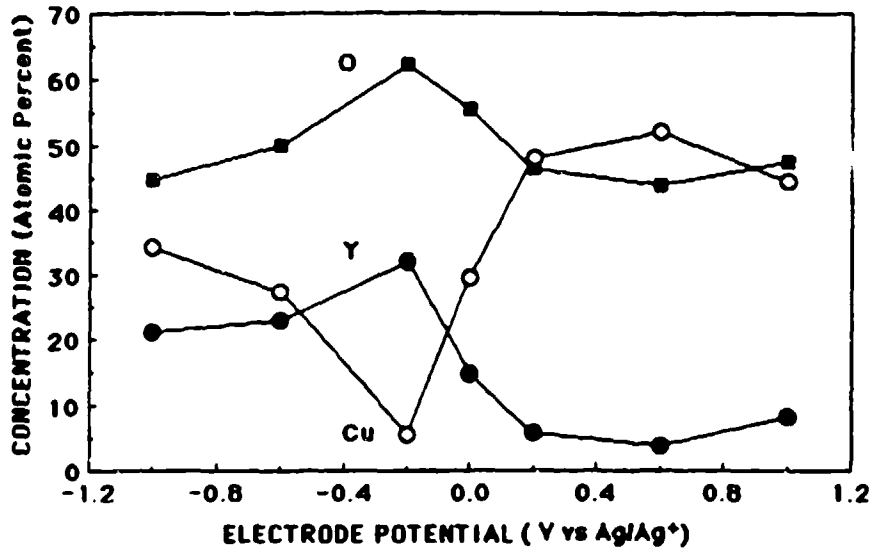

Fig. 7 Elemental surface composition determined by AES analysis for stationary Cu electrodes biased at various potentials after one minute on open circuit in eutectic Na-K nitrate melt (300°C) containing 30 mM Y^{3+} ion.

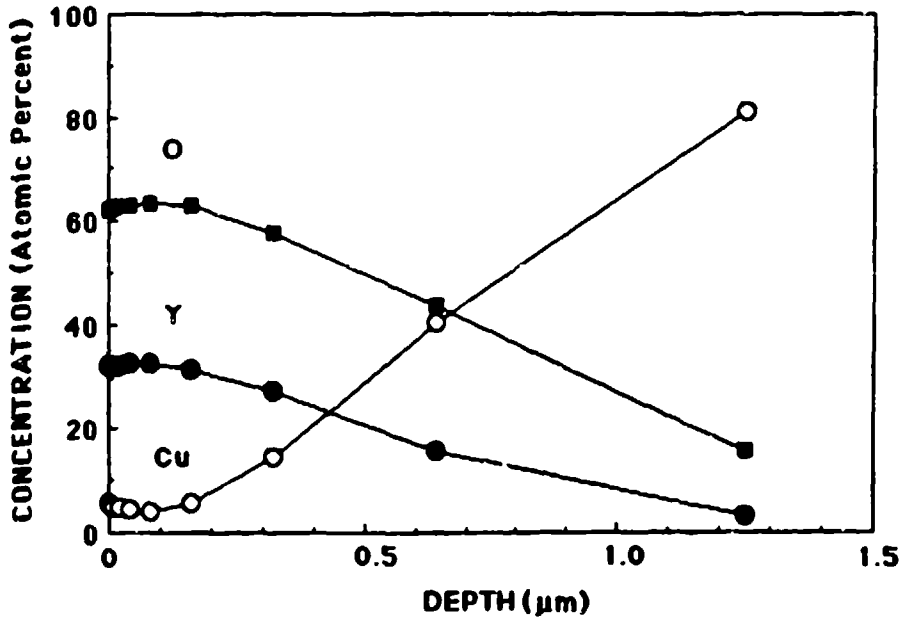

Fig. 8 AES depth profile for a stationary Cu electrode biased at -0.2 V for five minutes after one minute at open circuit in eutectic Na-K nitrate melt (300°C) containing 30 mM Y^{3+} ion.

As shown in Fig. 9, similar trends in surface composition were observed when Cu electrodes were introduced into the Y-containing melt with the potential applied. In this case, however, the oxide present at positive potentials is Cu_2O (2:1 Cu to O ratio) and the mixed oxide is depleted in Y at -0.6 V and Cu at more negative potentials. This is consistent with a more reduced Cu surface overall and deposition of Y_2O_3 on bare Cu at potentials around -1.0 V.

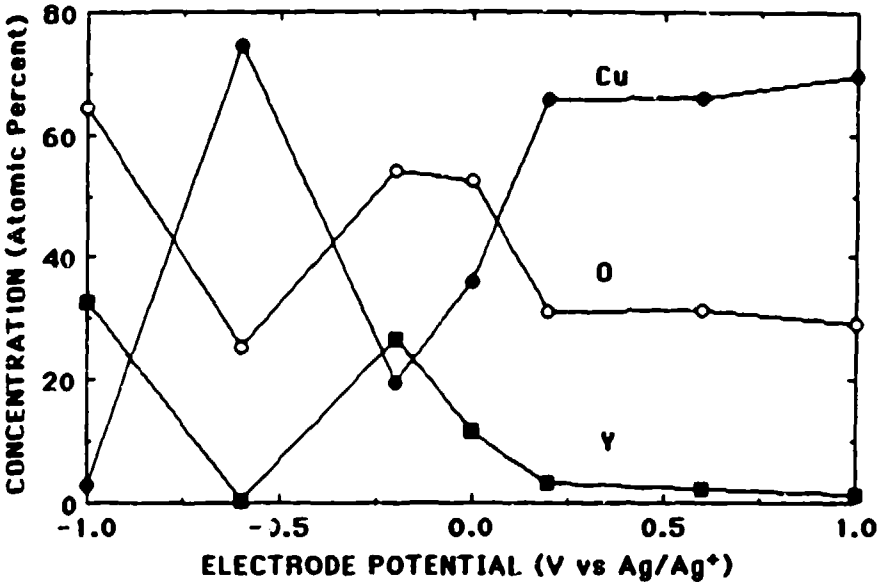

Fig. 9 Elemental surface composition determined by AES analysis for stationary Cu electrodes introduced with various potentials applied into eutectic Na-K nitrate melt (300°C) containing 30 mM Y^{3+} ion.

Mixed Yttrium-Barium-Copper Oxides

Similar experiments with equilibrated and un-equilibrated Cu electrodes were performed in melts containing both Y^{3+} and Ba^{2+} ions. The only conditions under which Ba was included in the surface oxide were for the equilibrated electrode at very negative potentials. Figure 10 shows the AES depth profile for the equilibrated Cu electode at -1.0 V in a melt containing 30 mM Y^{3+} and 90 mM Ba^{2+} ions. In this case, the surface oxide was predominantly Y_2O_3 but

contained as 1-3 atom percent barium distributed throughout the bulk surface oxide layer.

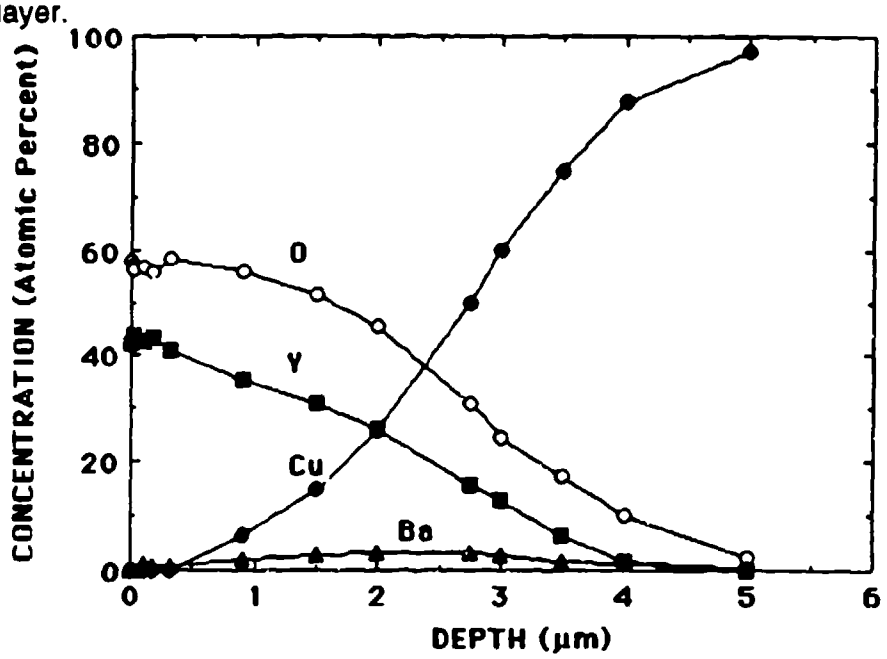

Fig. 10 AES depth profile for a stationary Cu biased at -1.0 V for five minutes after one minute at open circuit in eutectic Na-K nitrate melt (300°C) containing 30 mM Y^{3+} and 90 mM Ba^{2+} ions.

To verify the composition of the Y and Cu oxides, a specimen was deposited at -0.75 V on a rotating Pt electrode from a melt containing 10 mM Y^{3+}, 40 mM Cu^{2+} and 20 mM Ba^{2+} ions. No barium deposition was expected or observed at this potential. A scanning electron microroscopic study revealed that the deposit was comprised of small nodules (about 0.5 μm in diameter), indicative of diffusion controlled deposition. Figure 11 shows the x-ray spectrum for the material scraped from the electrode. The prominent peaks for both Y_2O_3 and CuO are evident.

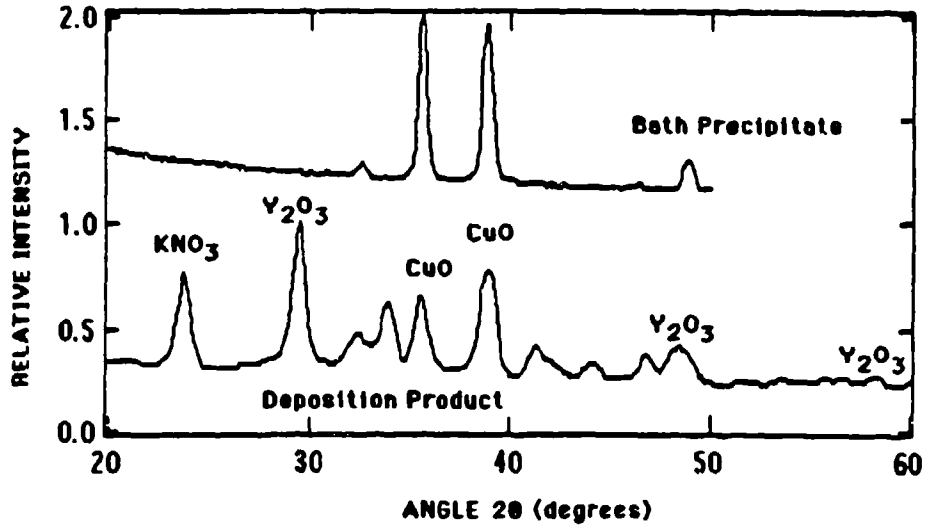

Fig. 11 X-ray diffraction spectrum of the deposit obtained on a Pt rotating disk electrode (600 rpm) at -0.75 V in eutectic Na-K nitrate melt (300°C) containing 10 mM Y^{3+}, 40 mM Cu^{2+} and 20 mM Ba^{2+} ions.

Cobalt Oxide Deposition

The likelihood that perovskites, specifically cobaltates, might be deposited from nitrate melts was established by demonstrating the deposition of cobalt oxide. As shown in Fig. 12, voltammograms at a Pt electrode in a melt containing anodically injected Co ions exhibit the same features at approximately the same voltages as those observed for Cu^{2+} ion. These are a diffusion-limited deposition plateau negative of 0.2 V, a superimposed anodic peak at about 0.0 V on the anodic voltage scan, and two anodic peaks associated with dissolution of the deposit. Note that these features are somewhat ill-defined in Fig. 12 since the Co^{3+} ion concentration in the melt is relatively high. As indicated by the x-ray diffraction scan in Fig. 13, the black deposit obtained on a Pt rotating disk electrode at -0.75 V from a melt containing 50 mM Co^{3+} ion is Co_3O_4. Since the average Co oxidation state in the oxide is 2.7, the melt species is presumed to be Co^{3+} ion (which undergoes partial reduction during the oxide deposition process).

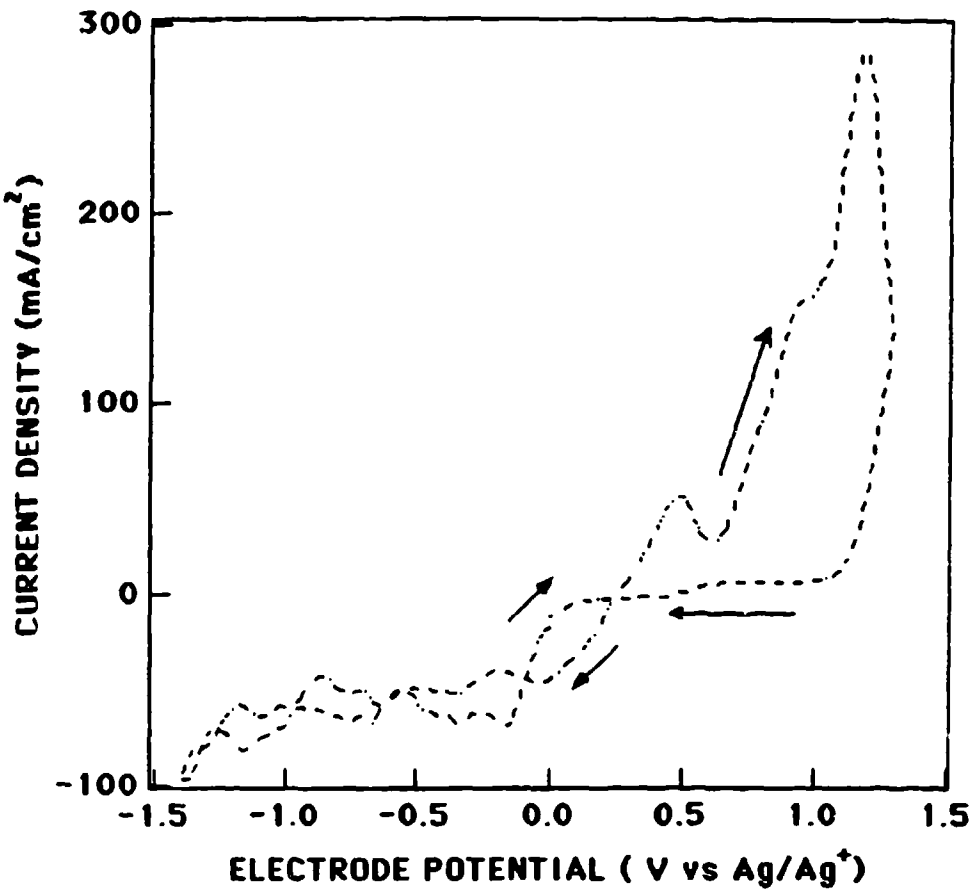

Fig. 12 Cyclic voltammograms (0.3 V/s) for a Pt rotating disk electrode (600 rpm) in eutectic Na-K nitrate melt (300° C) containing 100 mM Co^{3+} ion.

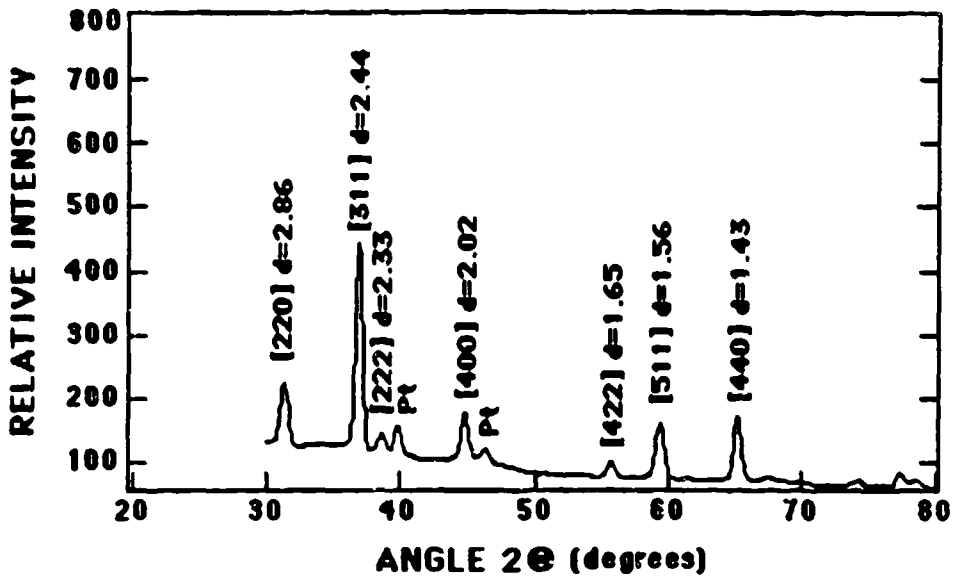

Fig. 13 X-ray diffraction scan for the deposit obtained on a Pt rotating disk electrode (600 rpm) at -0.75 V in eutectic Na-K nitrate melt (300°C) containing 50 mM Co^{3+} ion.

Mixed Oxide Compound Deposition Considerations

Figure 14 summarizes the available onset potential data for the electrochemical reactions pertinent to metal oxide deposition from the eutectic Na-K nitrate melt (references are given in brackets). Onset voltages have been used to minimize ambiguities but a precision of better than ±0.1 V cannot be expected since values were sometimes taken from journal figures and reactant concentrations, solution mass transport, voltage sweep rates, and temperature were somewhat variable. Generally, data are for reactant concentrations between 20 and 100 mM, stationary or slowly rotating Pt electrodes (0-600 rpm), sweep rates of 0.3-0.5 V/s, and temperatures of 250-300°C (unless otherwise noted).

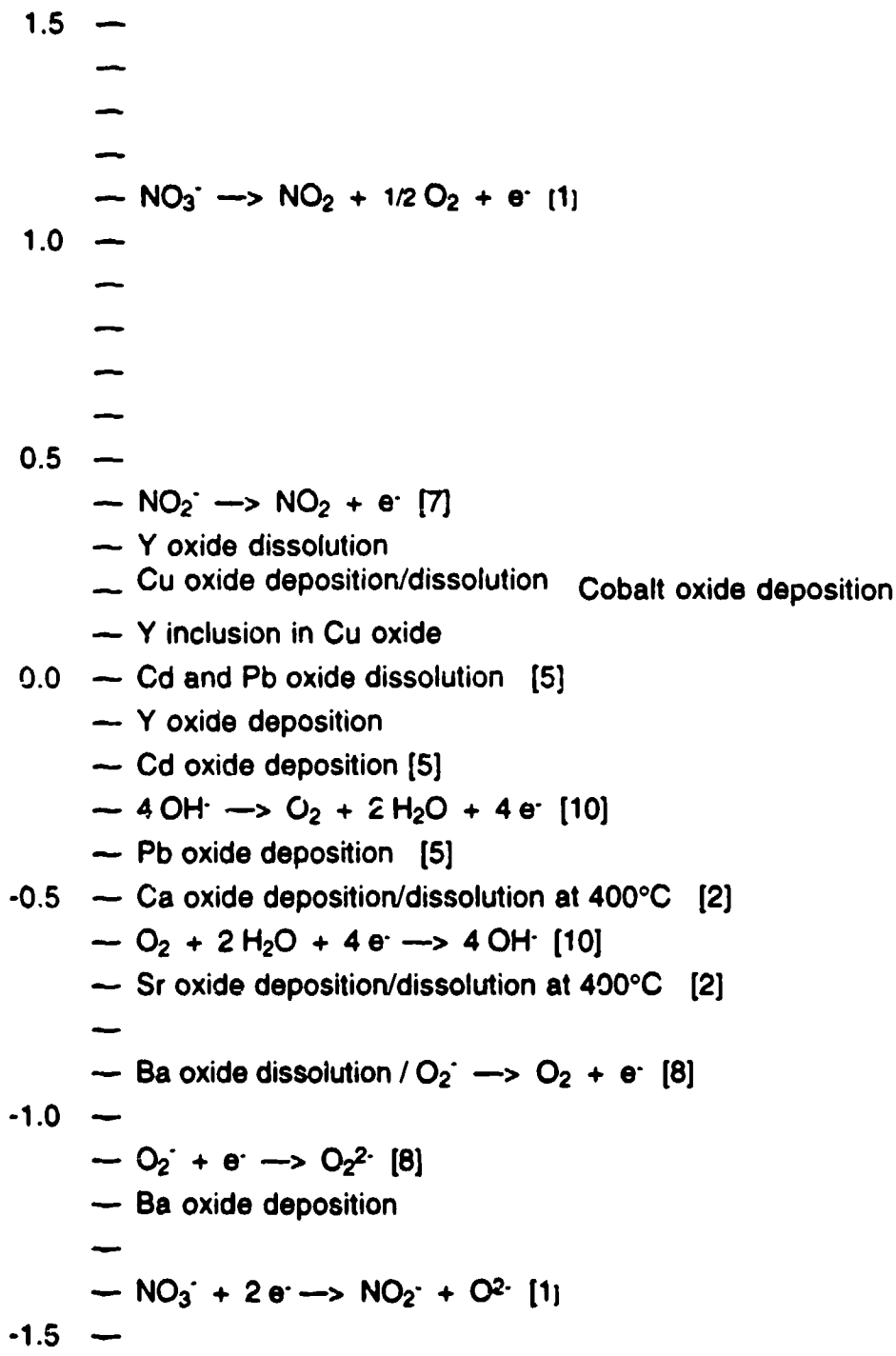

Fig. 14 Scale of onset potentials vs Ag/Ag^+ (0.07 M) for eutectic Na-K nitrate melt background reactions at 230°C, and metal oxide deposition processes at 300°C (this work) or 250°C (referenced work except [2]).

It is clear that the deposition potentials are sufficiently separated to permit metallic oxides to be selectively deposited in many cases. On the other hand, direct codeposition of some metallic oxides is also possible, particularly when compound formation occurs so that the potential for deposition of the more electropositive metal ion is shifted in the positive direction. This is apparently the case for Cu-Y oxides since Y is included in the Cu oxide at potentials positive of the Y deposition potential on platinum.

It is also evident from Fig. 14 that the electrochemical reactions involving oxygen species in the absence of water occur at very negative potentials and provide great flexibility in controlling the oxidizing power of the melt at the electrode surface. Note that the predominant melt oxygen species, superoxide (O_2^-), can be electrochemically oxidized to oxygen (O_2) or reduced to peroxide (O_2^{2-}), and oxide (O^{2-}) can be produced by reduction of nitrate (NO_3^-). For example, in a melt for which the bulk concentration of oxygen species had been minimized, the surface could be enriched in oxide (O^{2-}) by momentarily stepping the voltage negative of -1.4 V, and the oxide layer could then be converted to peroxide (O_2^{2-}), superoxide (O_2^-) or oxygen (O_2) by stepping the voltage positively to the appropriate value. Of course, the exact potentials required to effect these cor ions would depend on the substrate material (values given in Fig. 14 are for Pt).

SUMMARY AND CONCLUSIONS

Cathodic metal oxide electrodeposition from Na-K nitrate melts is a quite general phenomenon involving reduction of the metal nitrato complexes. Oxide deposition of Cu as CuO, Y as Y_2O_3, and Co as Co_3O_4 has been confirmed by AES and x-ray diffraction analyses. Anodic stripping of the Ba deposit occurs with large overvoltage (0.3 V) relative to the deposition potential, suggesting that the deposit is also an oxide in this case. The available data indicate that the nitrate melt system offers a wide range of possibilities for depositing both singe and mixed metallic oxides.

ACKNOWLEDGEMENT

This work was performed under DARPA Contract No. N00014-90-C-0225, which was administered by the Office of Naval Research.

REFERENCES

1. H. S. Swofford and H. A. Laitinen, J. Electrochem. Soc. 110, 814 (1963)

2. S. Sternberg and T. Visan, Electrochim. Acta 26, 75 (1981)

3. M. H. Miles, G. E. McManis and A. N. Fletcher, Proc. 4th Int. Symp. Molten Salts, ed. M. Blander, Electrochem. Soc. Vol. 86-2, p. 662 (1984)

4. M. H. Miles, G. E. McManis and A. N. Fletcher, Proc. 5th Int. Symp. Molten Salts, ed. M. L. Saboungi, K. Johnson, D. S. Newman and D. Inmen, Electrochem. Soc. Vol. 86-1, p. 234 (1986)

5. M. H. Miles, Electrochemica Acta, 32(2), 247(1987)

6. D. M. Tench, M. W. Kendig, S. Jeanjaquet, "Electrodeposition of Copper Oxide from the Eutectic Sodium-Potassium Nitrate Melt", submitted to J. Electrochem. Soc.

7. P. G. Zambonin and J. Jordan, J. Am. Chem. Soc. 89, 6365 (1967)

8. P. G. Zambonin and J. Jordan, J. Am. Chem. Soc. 91, 2225 (1969)

9. P. G. Zambonin and A. Cavaggioni, J. Am. Chem. Soc. 93, 2854 (1971)

10. P. G. Zambonin, J. Electroanal. Chem. 33, 243 (1971)

11. P. G. Zambonin, J. Electroanal. Chem. 45, 451 (1973)

12. P. G. Zambonin, J. Phys. Chem. 78, 1294 (1974)

13. J. M. Schlegel and D. Priore, J. Phys. Chem. 78, 2841 (1972)

14. J. D. Burke and D. H. Kerridge, Electrochim. Acta 19, 251 (1974)

15. P. G. Zambonin, Anal. Chem. 43, 1571 (1971)

16. L. G. Boxall and K. E. Johnson, Anal. Chem. 40, 831 (1968)

17. Phi Handbook of Auger Electron Spectroscopy

18. A. Conte, Electrochim. Acta 11, 1579 (1966)

19. T. Notoya, Denki Kagaku 41, 779 (1973)

SUPPLEMENTARY

INFORMATION

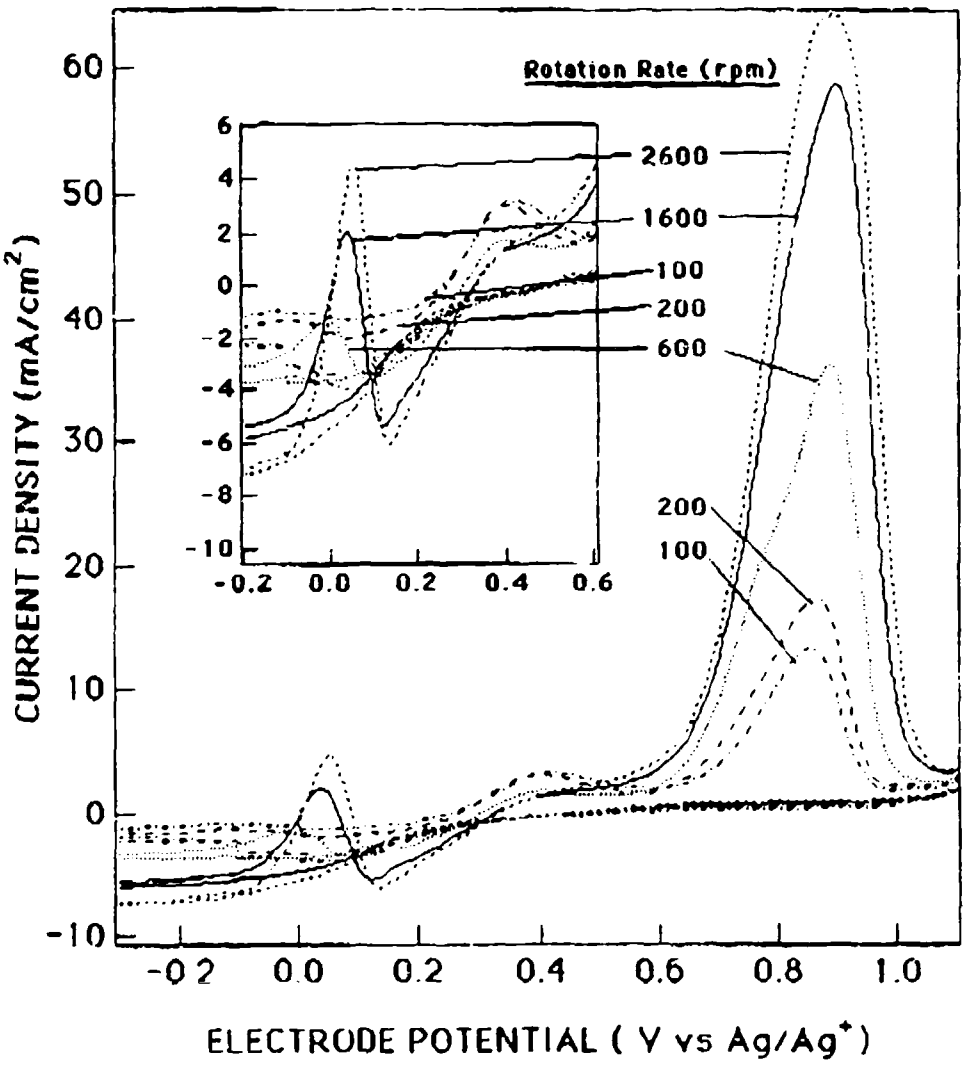

Fig. 9 Effect of rotation rate on the cyclic voltammetric behavior (0.3 V/s between -1.1 and 1.2 V) of a Pt disk electrode in eutectic Na-K nitrate melt (300°C) containing 10 mM Cu^{2+} ions.